U.S. DEPARTMENT OF COMMERCE/Environmental Science Services Administration

Technical Memorandum

INSTITUTES FOR ENVIRONMENTAL RESEARCH

IERTM-NSSL-29

NOTES ON THUNDERSTORM MOTIONS, HEIGHTS, AND CIRCULATIONS

T. W. Harrold
W. T. Roach
Kenneth E. Wilk

NATIONAL SEVERE STORMS LABORATORY
NORMAN, OKLAHOMA
November 1966

ENVIRONMENTAL SCIENCE SERVICES ADMINISTRATION

INSTITUTES FOR ENVIRONMENTAL RESEARCH

NATIONAL SEVERE STORMS LABORATORY TECHNICAL MEMORANDA

The National Severe Storms Laboratory, Norman, Oklahoma, in cooperation with other goverment groups, and with units of commerce and eduction, seeks to increase understanding of severe local storms, to improve methods for detecting these storms and for measuring associated meteorological parameters, and to promote the development and applications of weather radar.

Reports by the cooperating groups are printed as NSSL Technical Memoranda, a subseries of the ESSA Technical Memorandum series, to facilitate prompt communication of information to vitally interested parties and to elicit their constructive comments. These Memoranda are not formal scientific publications.

The NSSL Technical Memoranda, beginning with No. 28, continue the sequence established by the U. S. Weather Bureau National Severe Storms Project, Kansas City, Missouri. Numbers 1-22 were designated NSSP Reports. Numbers 23-27 were NSSL Reports, and 24-27 appeared as a subseries of Weather Bureau Technical Notes.

Reports in this series are available from the Clearinghouse for Federal Scientific and Technical Information, U. S. Department of Commerce, Sills Bldg., Port Royal Road, Springfield, Virginia 22151.

No. 1 National Severe Storms Project Objectives and Basic Design. Staff, NSSP. March 1961.
No. 2 The Development of Aircraft Investigations of Squall Lines from 1956-1960. B. B. Goddard.
No. 3 Instability Lines and Their Environments as Shown by Aircraft Soundings and Quasi-Horizontal Traverses. D. T. Williams. February 1962.
No. 4 On the Mechanics of the Tornado. J. R. Fulks. February 1962.
No. 5 A Summary of Field Operations and Data Collection by the National Severe Storms Project in Spring 1961. J. T. Lee. March 1962.
No. 6 Index to the NSSP Surface Network. T. Fujita. April 1962.
No. 7 The Vertical Structure of Three Dry Lines as Revealed by Aircraft Traverses. E. L. McGuire. April 1962.
No. 8 Radar Observations of a Tornado Thunderstorm in Vertical Section. Ralph J. Donaldson, Jr., April 1962.
No. 9 Dynamics of Severe Convective Storms. Chester W. Newton. July 1962.
No. 10 Some Measured Characteristics of Severe Storm Turbulence. Roy Steiner and Richard H. Rhyne. July 1962.
No. 11 A Study of the Kinematic Properties of Certain Small-Scale Systems. D. T. Williams. October 1962.
No. 12 Analysis of the Severe Weather Factor in Automatic Control of Air Route Traffic. W. Boynton Beckwith. December 1962.
No. 13 500-Kc./Sec. Sferics Studies in Severe Storms. Douglas A. Kohl and John E. Miller. April 1963.
No. 14 Field Operations of the National Severe Storms Project in Spring 1962. L. D. Sanders. May 1963.
No. 15 Penetrations of Thunderstorms by an Aircraft Flying at Supersonic Speeds. G. P. Roys. Radar Photographs and Gust Loads in Three Storms of 1961 Rough Rider. Paul W. J. Schumacher. May 1963.
No. 16 Analysis of Selected Aircraft Data from NSSP Operations, 1962. T. Fujita. May 1963.
No. 17 Analysis Methods for Small-Scale Surface Network Data. D. T. Williams. August 1963.
No. 18 The Thunderstorm Wake of May 4, 1961. D. T. Williams. August 1963.
No. 19 Measurements by Aircraft of Condensed Water in Great Plains Thunderstorms. George P. Roys and Edwin Kessler. July 1966.
No. 20 Field Operations of the National Severe Storms Project in Spring 1963. J. T. Lee, L. D. Sanders, and D. T. Williams. January 1964.
No. 21 On the Motion and Predictability of Convective Systems as Related to the Upper Winds in a Case of Small Turning of Wind with Height. James C. Fankhauser. January 1964.
No. 22 Movement and Development Patterns of Convective Storms and Forecasting the Probability of Storm Passage at a Given Location. Chester W. Newton and James C. Fankhauser. January 1964.
No. 23 Purposes and Programs of the National Severe Storms Laboratory, Norman, Oklahoma. Edwin Kessler. December 1964.
No. 24 Papers on Weather Radar, Atmospheric Turbulence, Sferics, and Data Processing. August 1965.
No. 25 A Comparison of Kinematically Computed Precipitation with Observed Convective Rainfall. James C. Fankhauser. September 1965.
No. 26 Probing Air Motion by Doppler Analysis of Radar Clear Air Returns. Roger M. Lhermitte. May 1966.

(Continued on inside back cover)

U.S. DEPARTMENT OF COMMERCE ● John T. Connor, Secretary

ENVIRONMENTAL SCIENCE SERVICES ADMINISTRATION

Robert M. White, Administrator

Institutes for Environmental Research

George S. Benton, Director

Institutes for Environmental Research Technical Memorandum NSSL-29

NOTES ON THUNDERSTORM MOTIONS, HEIGHTS, AND CIRCULATIONS

T. W. Harrold
W. T. Roach
Kenneth E. Wilk

NATIONAL SEVERE STORMS LABORATORY
TECHNICAL MEMORANDUM NO. 29

NORMAN, OKLAHOMA
November 1966

The program at the National Severe Storms Laboratory involves the cooperative participation of many government agencies and other groups.

The papers in this report consider thunderstorm motions, height of thunderstorm tops, and selected features of the air circulation and dynamical properties of thunderstorms. The data were collected by personnel and equipment managed by NSSL and the Air Force Cambridge Research Laboratories, and analyzed by staff of NSSL and the British Meteorological Office. Analysis was aided by financial support from NASA and FAA.

A NOTE ON THE DEVELOPMENT AND MOVEMENT OF STORMS OVER OKLAHOMA ON MAY 27, 1965

T. W. HARROLD
Meteorological Office, Malvern, England

ABSTRACT

Two tornadic storms developed near the Texas-Oklahoma border on May 27, 1965. These storms diverged markedly for several hours, one moving 30° to the right and the other 30° to the left of the mean wind over the cloud depth. A detailed examination of the PPI radar data at 1-min. intervals showed that some individual cells, as well as the larger storm area, were diverging. The Kutta-Joukowski force is considered as a possible factor in the movement, and it is also noted that the movement to the right of the wind could have resulted from continuous propagation toward the moisture supply.

The highest storm top, as observed from an aircraft in the vicinity, was higher than that predicted from the parcel theory of convection. This may indicate a significant release of latent heat of fusion within the storm.

1. INTRODUCTION

Severe storms developed near the Texas-Oklahoma border during the early afternoon of May 27, 1965. The movement and some other features of these storms were considered sufficiently interesting to warrant some investigation.

2. SYNOPTIC SITUATION

At 0600 (times throughout this note are CST) relatively cool and dry air covered all of Oklahoma below about 700 mb., and winds in this layer were from an easterly quarter. Above 700 mb., winds were between west and southwest at all heights. During the morning, warmer moist air (dew point above 60°F.) moved north or northwest over Texas. This warm air, undercutting potentially cooler air above, and solar heating, permitted the development of thunderstorms. The surface chart for 1400 CST is shown in figure 1. The position of the radar echo at 1400 (the time of the first radar observations) is included in the figure. This storm was within a general area of surface convergence and on the axis of the dew point maximum. It is possible that the storm was initiated closer to the dry line, which is revealed by the marked drop in dew point southwest of Oklahoma, since the history of the echo before about 1400 is not known.

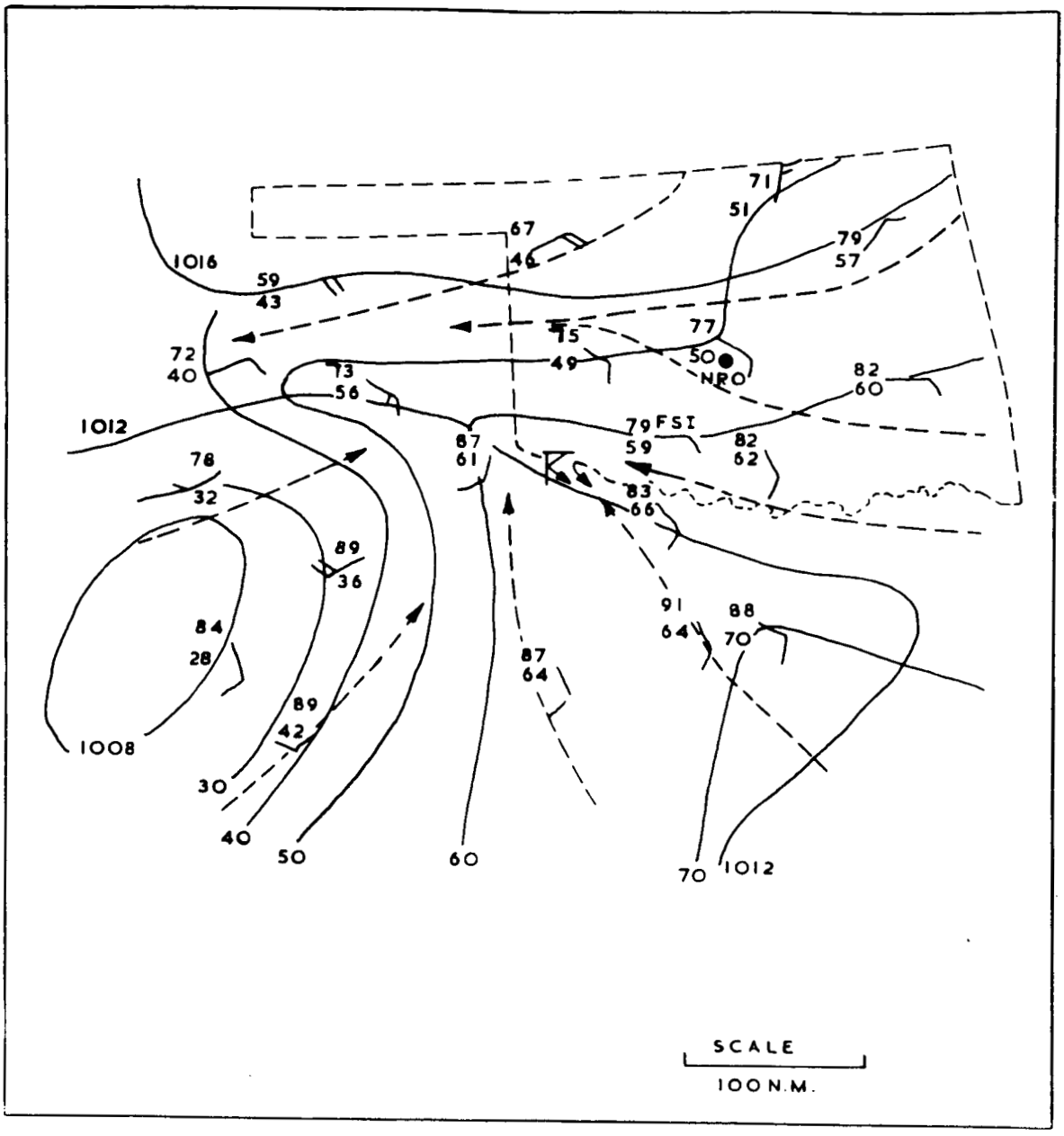

Figure 1. - Surface weather, 1400 CST, May 27, 1965, showing dry bulb temperature, dew point and wind at selected stations. Solid heavy lines are isopleths of dew point (10°F. intervals) and lighter solid lines are sea level isobars (4-mb. intervals). Dashed lines are surface streamlines. The positions of Norman (NRO) and Fort Sill (FSI) are also shown. ⇆ marks the position of the radar echo visible on the WSR-57 at Norman at 1400.

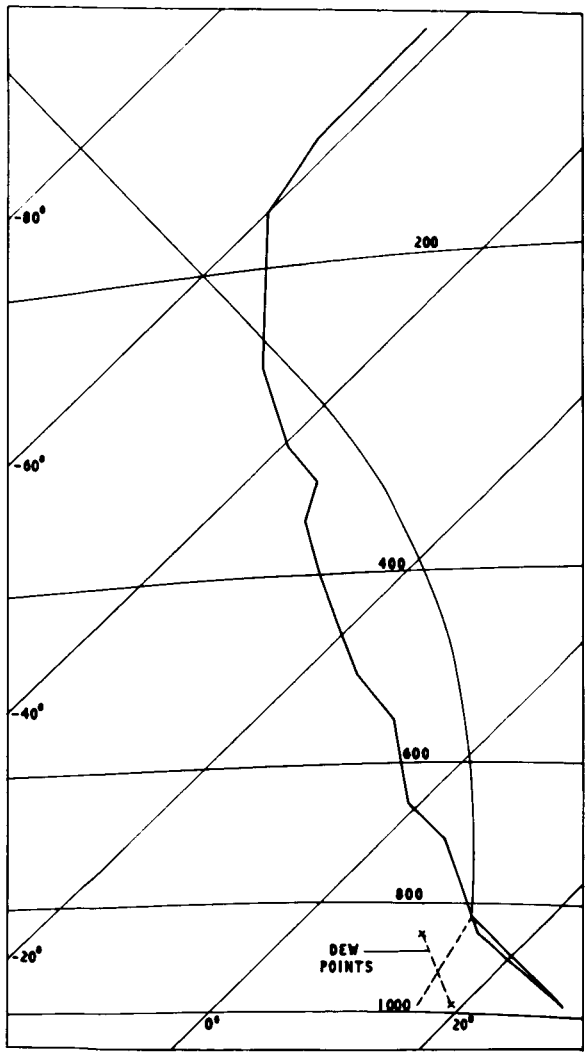

A tephigram of the conditions close to the storm is shown in figure 2. This ascent is an interpolation, based largely on Fort Sill soundings (40 n.mi. northeast of the storm at 1400) at 1200, 1430, and 1600 CST, but with the lowest levels modified to take into account the increase in temperature and dew point southwestward from Fort Sill. Assuming the "parcel theory" of convection, cloud tops could reach 49,500 ft.

Figure 2. - Temperature sounding in vicinity of storm at 1400. The ascent is based largely on the Fort Sill ascents at 1200, 1430, and 1600, but with the lowest levels modified to take into account the increase in temperature and dew point southwest from Fort Sill.

3. STORM MOVEMENT

Hourly positions of the radar echo are shown in figure 3. Reflectivity factor contours, traced from photographs of the integrated log contour display [4] of the WSR-57 at Norman (NRO), are at 10-db. intervals, starting with $Z = 30$ mm.^{6}/m^3. The mean hourly speeds of the two main complexes are also shown. The Fort Sill (FSI) hodograph at 1600 where heights are indicated in km., is included as an inset; the vector directed from the broken line to the origin of the polar diagram indicates the direction toward which the wind was blowing. Hodographs at 1200, 1430 and 1800 are similar to that at 1600.

The two storm areas diverged markedly, the separation of the cores increasing from about 20 n.mi. at 1415 to 100 n.mi. at about 1715. Neither storm moved with the mean wind over the cloud depth

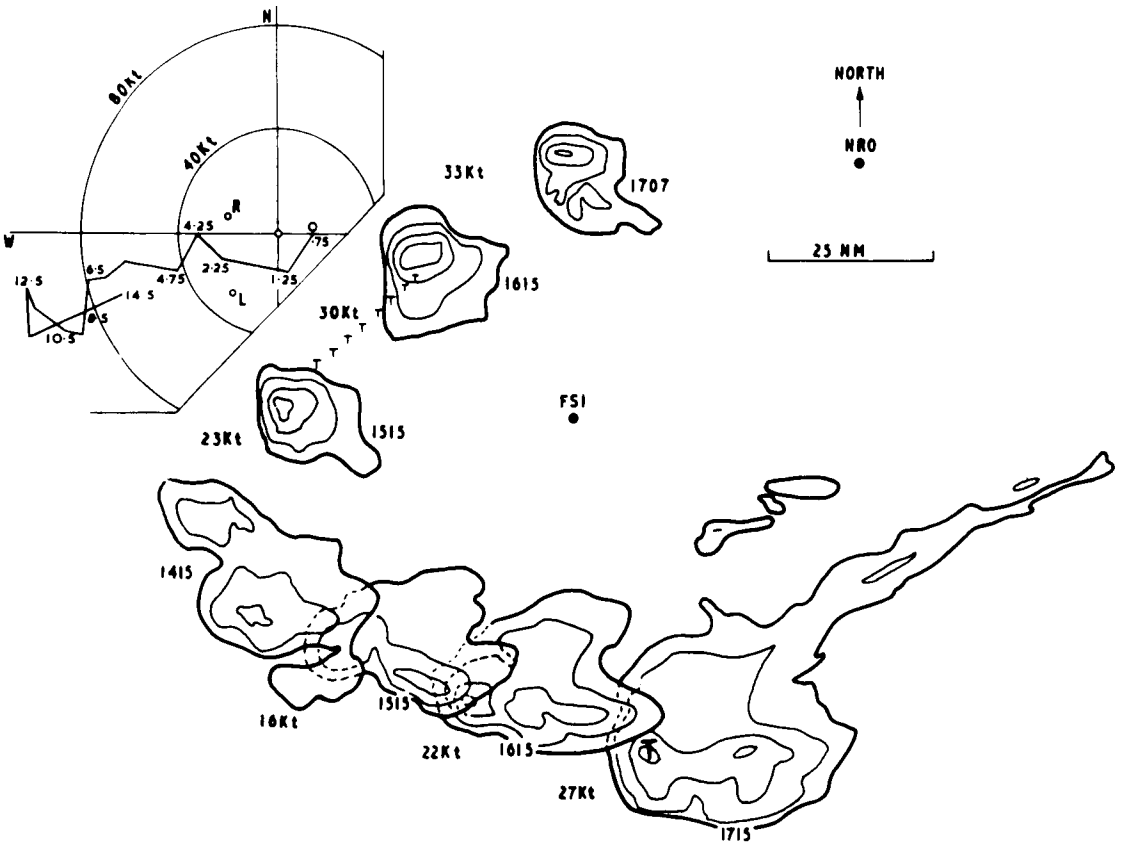

Figure 3. - Hourly positions of radar echoes observed from Norman, showing diverging storm tracks. Echo contours are at 10-db. intervals, starting at Z = 30 mm^6/m^3. Mean hourly speeds of the echo centers are included. T denotes the occurrence of a tornado (deduced from Storm Data, USWB, May 1965 and local press reports). The inset shows the Fort Sill hodograph at 1600, the heights on this diagram being in km. and the broken line passing through the azimuths from which the wind was blowing. The positions of storm R(290°/20 kt.) and storm L (220°/30 kt.) at this time are shown.

(which was from 255°), the northern storm moving to the left (henceforth termed storm L) and the southern one to the right (storm R) of the winds. Storm L moved somewhat more rapidly than storm R. Positions L and R are included in the hodograph on figure 3 to facilitate comparison with the wind field. This storm couplet remarkably resembles a system reported and illustrated by Newton and Fankhauser [6], whose formation occurred on May 24, 1962 at a place about 25 n.mi. west of this storm origin. These storms also resemble those discussed by Wilk elsewhere in this NSSL Report [7].

Marble-sized hail and a tornado (see fig. 3) were associated with storm L for part of its life. At least two tornadoes and baseball-

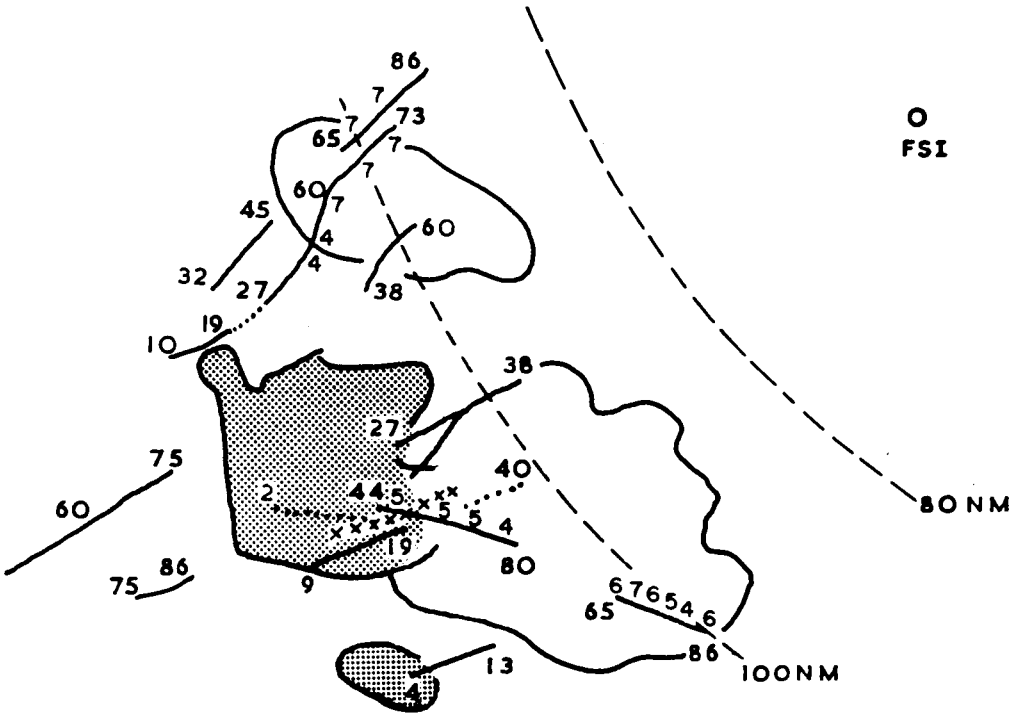

Figure 4. - Movement of cell centers, as identified by closed contour (s) on the integrated log contour display, 1400-1526. Lines show tracks of cells with the time in minutes after 1400 of the beginning and end of the cell life cycle. Echo intensities of the three strongest cells are also shown as small figures alongside the tracks, where 4 indicates $Z > 10^3$, $5 = Z > 3 \times 10^4$, and $7 = Z > 3 \times 10^4 mm.^6/m^3$. The shaded echo is that at 1400, the open echo that at 1500. Storm L did not exist at 1400 except possibly as the small protuberance on the northwest side of the main echo.

sized hail were reported from the vicinity of storm R. Storm L decayed rapidly after 1700, when it moved away from the supply of moist surface air, but storm R persisted for several hours.

The time scale on figure 3 is too coarse to determine whether individual cells, as well as the two complex masses, were moving or propagating in directions other than that of the mean wind. To determine this, an analysis of cell movement by means of integrated log contour photographs taken at 1-min. intervals,has been made for the 1-1/2 hours after 1400. The position of a cell was taken as the center of the innermost closed contour. The time interval of 1 min. between contoured pictures is shorter than that available to most other workers who have assessed cell movements. Consequently, the chance of unnoticed development of a new cell close to an old one is reduced. The movement of individual cells is shown on figure 4. The two-digit figures along

each track denote the time in minutes after 1400. Also, along the tracks of the three strongest cells the echo intensity of the center is shown as a number between 4 and 7, the corresponding values of Z being greater than 10^3, 3×10^3, 10^4, and 3×10^4 $mm.^6/m.^3$, respectively. The extent of the echo at 1400 and 1500 is also shown.

Storm L was not in existence at 1400, except possibly as a small northwest extension of storm R. Range markers show distance from the radar at Norman. (At 100 n.mi. range the 1.8° wide beam of the WSR-57 would resolve only those cells separated by more than about 1-1/2 n.mi. in azimuth.) The figure shows that many of the cells were moving or propagating from about 250° but that there were definite exceptions among the strongest echoes. Storm L started veering to the left of the winds less than 10 min. after the first closed contour appeared and generally moved from about 225°. Many of the identifiable centers of storm R moved or propagated to the right of the winds, from about 285°, and this was the case even when this storm was in a quiet phase with peak reflectivity of about 10^3 $mm.^6/m.^3$ It is interesting to note that the resultant motion of storms L and R combined is from 250° which is about the direction of the steering wind.

It has been suggested (e.g. Byers [2], Fujita [3]) that the Kutta-Joukowski force might result in storms moving either to the left or right of the steering wind. A solid cylinder rotating inside a perfect fluid of density ρ and uniform flow of speed u receives a force F toward the side of the highest resultant speed defined by superposition of rotational and translational speeds. This force is $F = \rho u \Gamma$ per unit length of the cylinder, where Γ denotes the circulation around the rotating cylinder. Thus, if the storm can be considered analogous to a solid rotating cylinder[1], a cyclonically rotating storm would move to the right of the wind field, and an anticyclonically rotating storm to the left. To determine whether this effect might have been the cause of the movement of the storms on May 27, the radar data between 1400 and 1445 were investigated to determine whether any rotation was apparant. Although there was no definite indication of rotation, the cells near the center of storm R at about 1400 tended to move more slowly than the echoes near both the north and south boundaries, though only by about 5 kt., which cannot be considered outside the limits of probable error in the measurements. If this was a real effect, it suggests the possibility of a small cyclonic shear on the south side and anticyclonic shear on the north side of the storm and the resulting Kutta-Joukowski force would tend to steer a cell on the south side to the right, as in fact occurred. Thus if we approximate storm L or R to a cylinder of diameter D and height h, the circumference rotating with a mean tangential velocity v, and consider this cylinder to be imbedded in a uniform horizontal flow of speed u, we have

---

[1] The concept of the May 27 storm as a barrier to the ambient flow is reinforced by aircraft observations of very large temperature gradients in the clear air near the storm [1].

$$\frac{\text{K-J Force}}{\text{horiz. wind force}} = \frac{\rho u \Gamma h}{\frac{1}{2}\rho u^2 Dh} = \frac{2\pi v}{u} .$$

assuming a drag coefficient of unity. (Malkus [5] has presented a discussion of the form drag on clouds.) If we put u = 50 kt., v = 2-1/2 kt., the estimated K-J force is about 0.3 of the estimated drag of the ambient wind, enough to move the storm about 15° to the right of the steering flow. The observed larger deflection would be explained if the drag coefficient applicable to the cloud was about 0.50 rather than unity.

The direction of movement of L coincides with the wind at about the 2-km. height. However, the speed of movement was twice the wind speed (fig. 3, inset) and it is evident that no ordinary steering mechanism is applicable to this storm, which extended above a height of 12 km.

An alternative explanation of the movement of storm R is that it was continuously propagating toward the moisture supply. This cannot apply to storm L.

4. STORM TOPS

Storm L was within RHI range (80 n.mi. from Norman) for much of its life. The radar top was about 40,000 ft. initially, but decreased as the storm moved northward. Pulsations of the storm top were noted, suggesting that a completely steady state had not been reached. The west cell of storm R, on the other hand, had a persistent top between 50,000 and 55,000 ft., as reported from a Canberra flying at 45,000 ft. in the vicinity of this storm [1]. The Oklahoma City WSR-57 weather radar reported the top exceeding 60,000 ft. but since the storm was 120 n.mi. from this radar, the effects of beamwidth and sidelobes make this figure unreliable. The top was outside the range of the Norman RHI. Although it is difficult to determine the height of a storm top from an aircraft, it seems probable that the top of this storm exceeded the 49,500 ft. predicted by the parcel theory (fig. 2). W. T. Roach (private communication) has previously remarked on a tendency for some large storm tops to exceed the height expected from the parcel theory. Since figure 2 is representative of conditions close to the storm some other source of energy must have increased the height of the storm. One possibility is the conversion of the horizontal kinetic energy of the inflow to vertical air motion, but in practice this could not appreciably increase the top. On this occasion the surface air was moving at about 40 kt. relative to the storm. The resulting energy of 2×10^6 erg/unit mass of air would increase the storm top by less than 1,000 ft. A more likely source of energy is the release of latent heat as the water drops in the storm freeze. The saturated adiabatics on the tephigram are with respect to liquid water at all temperatures and do not include this possible source of energy. If we assume a liquid water content of

5 gm./m.^{3}, which is reasonable for at least portions of a large storm, then, on freezing, 3×10^7 erg/unit mass of air are liberated. This would be sufficient to increase the storm top by several thousand feet.

5. SUMMARY

This note has described the motion of two neighboring storms, one of which moved 30° to the right and the other 30° to the left of the mean wind direction over the cloud depth. The Kutta-Joukowski force is considered to be a possible factor in the movement but the analysis does not permit firm conclusions concerning this. An alternative explanation that storm R was continuously propagating toward the moisture supply seems feasible, but no complete explanation of the observed motion of storm L has been offered. It is suggested that the release of latent heat of fusion in storm R enabled the top to exceed that predicted by the parcel theory of convection.

REFERENCES

1. Burns, A. and T. W. Harrold, "An Atmospheric Disturbance Encountered by a Canberra over Storms at Oklahoma May 27, 1965," NSSL Report (in preparation).

2. Byers, H., Non-Frontal Thunderstorms. Miscellaneous Report No. 3, Meteorological Dept., University of Chicago, 1942.

3. Fujita, T., "Formation and Steering Mechanisms of Tornado Cyclones and Associated Hook Echoes," Monthly Weather Review, vol. 93, No. 2, February, 1965, pp. 67-78.

4. Lhermitte, R. and Kessler, E., "A Weather Radar Signal Integrator." National Severe Storms Laboratory Tech. Memo No. 2, Norman, Okla.

5. Malkus, J.S., "The Slopes of Cumulus Clouds in Relation to External Windshear," Quarterly Journal Royal Meteorological Society, vol. LXXVIII, No. 338, 1952, pp. 530-542.

6. Newton, C. W. and Fankhauser, J. C., "On the Movements of Convective Storms, with Emphasis on Size Discrimination in Relation to Water Budget Requirements," Journal of Applied Meteorology, vo.. 3, No. 6, Dec. 1964, pp. 651-668. (See fig. 15)

7. Wilk, K. E., "Motion and Intensity Characteristics of Severe Thunderstorms on April 3, 1964,"

MOTION AND INTENSITY CHARACTERISTICS OF THE SEVERE THUNDERSTORMS OF APRIL 3, 1964

KENNETH E. WILK
National Severe Storms Laboratory, Norman, Oklahoma

ABSTRACT

Objective techniques are used for analysis of five severe thunderstorms which occurred on April 3, 1964 in Oklahoma and Texas. The radar reflectivities and velocities of the storms are presented and the differences among storms are discussed. The average motion of all storms corresponds to the mean layer wind from the surface to 8 km; however, the range of individual velocities is as large as the mean. Differences in direction of motion rather than speed, contribute most to this variability.

Although velocities vary from storm to storm, the velocity of the individual storm is conservative and provides a suitable basis for short term forecasting. Probability forecasting by objective extrapolation of individual storm positions is discussed.

The variability of the storm motions is viewed with respect to recent theories relating storm translation, rotation, and water budget to the environmental wind.

1. INTRODUCTION

Weather radar is a powerful probe for determining the distribution and motion of convective storms. Numerous researchers have described a wide variety of storm motions. Anomalies coincident with severe weather phenomena include convergent or divergent tracks, and sudden changes in echo velocity. Recent studies of a more quantitative nature have shown that individual storm motion sometimes departs greatly from the mean layer environmental wind and may be related to the rotation and development of the storm. These studies are discussed in the final section of this paper.

The radar reflectivity factor Z is an indication of a storm's severity [1, 2, 3]. This paper describes the translational properties of a family outbreak of severe thunderstorms derived from an objective analysis of storm reflectivities.

2. THE STORMS OF APRIL 3, 1964 - THE SYNOPTIC PATTERN

The macroscale, surface pressure pattern which existed prior to the development of these severe thunderstorms in Oklahoma and Texas was characteristic of spring storms, with a major cyclone covering much of the central United States. The pattern was atypical, however, in that the low pressure center retrograded to the southwest during the 18-hr. period prior to the development of the severe storms. Figures 1 and 2 illustrate the translation of the pressure system and the characteristics of the air masses involved. By 1200 CST on April 3 the stage was set for thunderstorm activity in northern Texas and

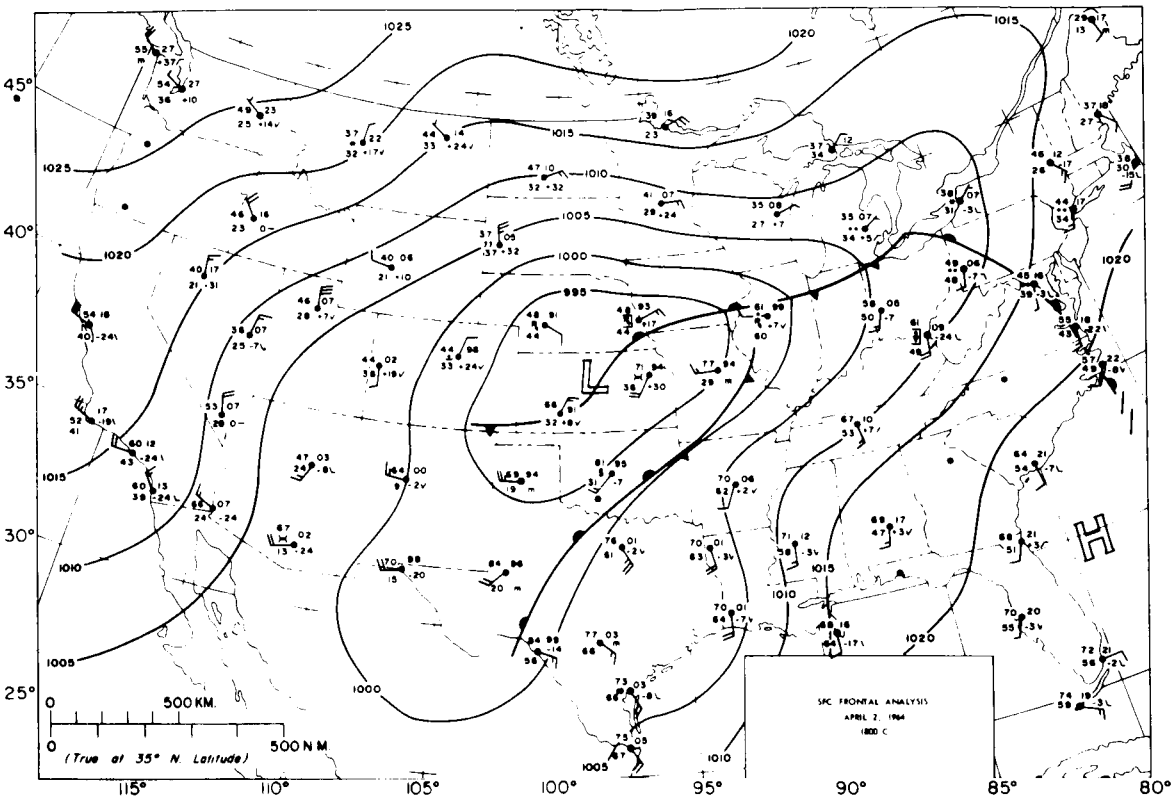

Figure 1. - Surface analysis, April 2, 1964, 1800 CST

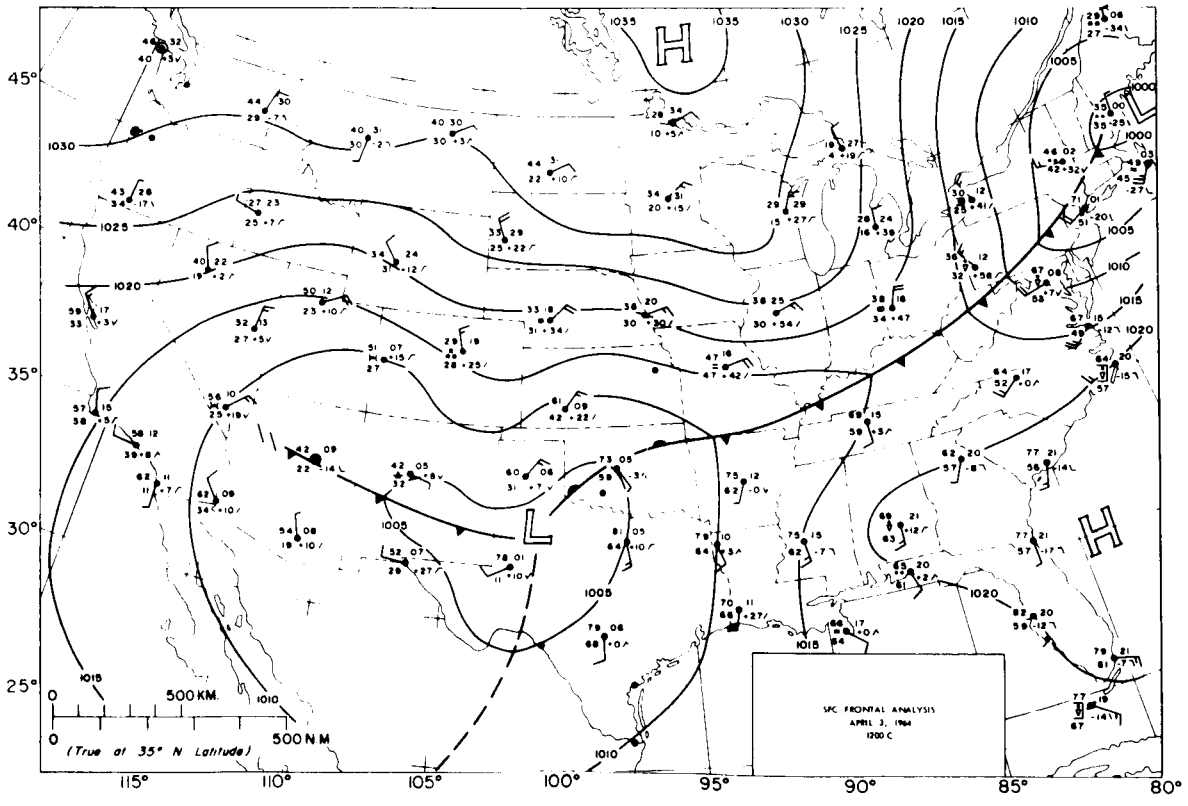

Figure 2. - Surface analysis, April 3, 1964, 1200 CST

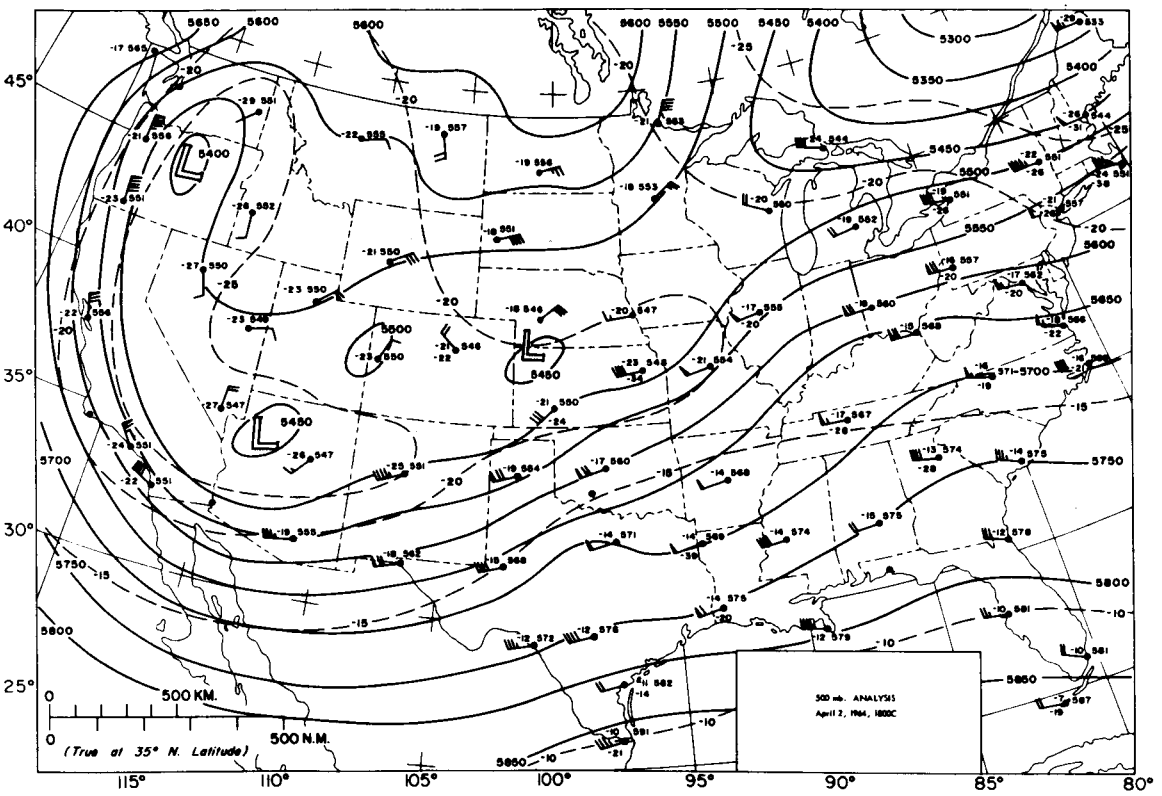

Figure 3. - 500-mb. analysis, April 2, 1964, 1800 CST.

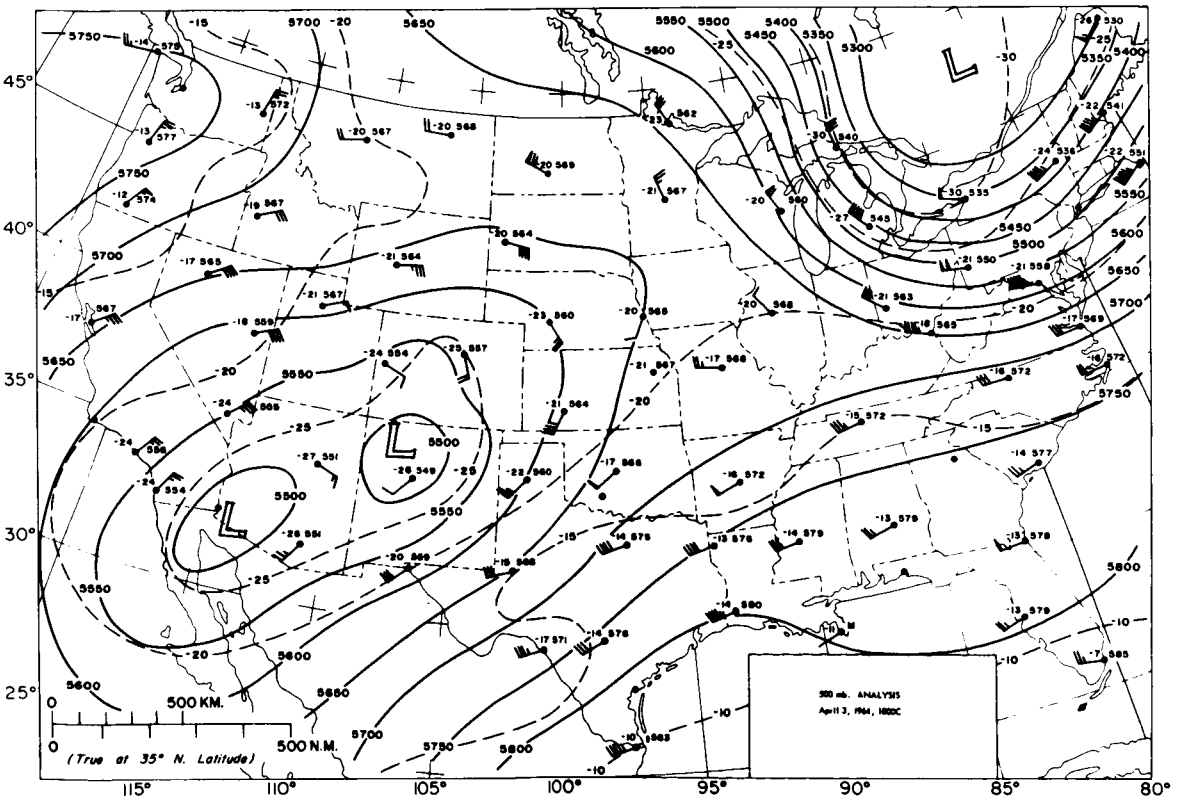

Figure 4. - 500-mb. analysis, April 3, 1964, 1800 CST.

southern Oklahoma with a convergent flow of moist Gulf air rapidly increasing the convective instability in the warm sector.

At the 500-mb. level, thermal advection shown in figure 3 was followed by the formation of the closed Low over New Mexico, shown in figure 4. The double-Low was associated with diffluent flow in the upper troposphere over Oklahoma.

By 1800 CST on April 3 (midway through the severe storm period) the winds over Oklahoma veered smoothly with height, changing from southeast at the surface to southwest at 500-mb. and to west-southwest at 300-mb. The mean wind analysis for the layer from the surface to 8 km is shown in figure 5. This average flow closely approximates the mean echo motion vector. The variance of the wind velocity over Oklahoma is about 50 percent of the mean; the mean layer wind over south-central Oklahoma is 13 $m.sec.^{-1}$ from 225 deg.

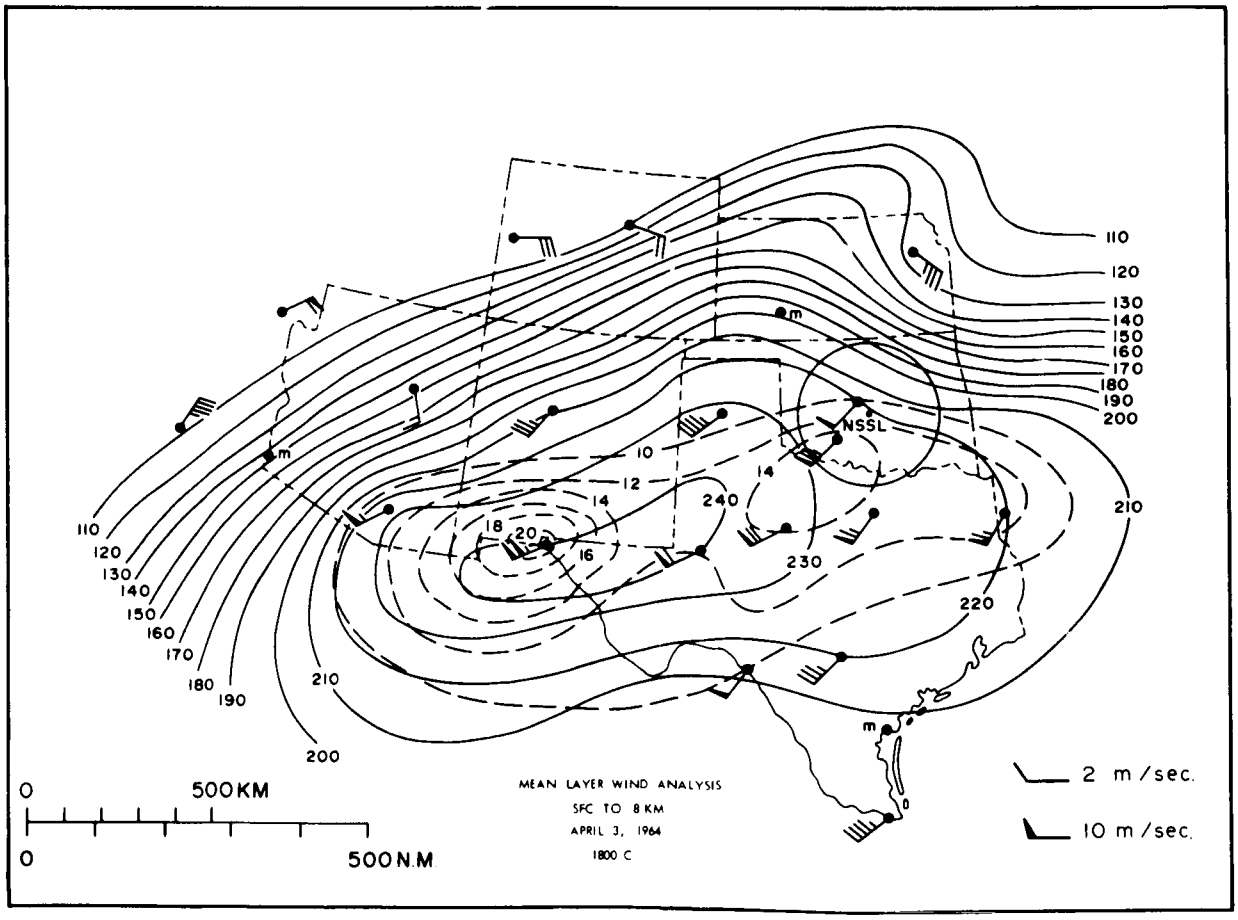

Figure 5. - Mean layer wind analysis, surface to 8 km., April 3, 1964, 1800 CST.

3. THE STORM (ECHO) MOTION FIELD

The objective analysis techniques used at the National Severe Storms Laboratory (NSSL) for studying echo characteristics are modeled after methods originated at Travelers Research Center by Kessler and Russo [4] and modified by Wilson [5]. Echo intensity contours are transformed to reflectivity integers which are referenced to a rectangular coordinate field of 6400 (2.5 n. mi. x 2.5 n. mi.) grid points. The grid covers the geographic area within 100 n. mi. radius of the radar location. The NSSL WSR-57 radar sampling scheme provides approximately six composite displays per hour. The original 35-mm. scope photographs consist of a repetitious series of step attenuation and antenna tilt angles. After the traced intensity contours are transferred to punch cards, the cataloged integers are computer processed to provide a statistical description of storm parameters, including coverage, average intensity, intensity variance, and velocity.

The digitization of the scope photographs is illustrated in figures 6 and 7. Figure 6

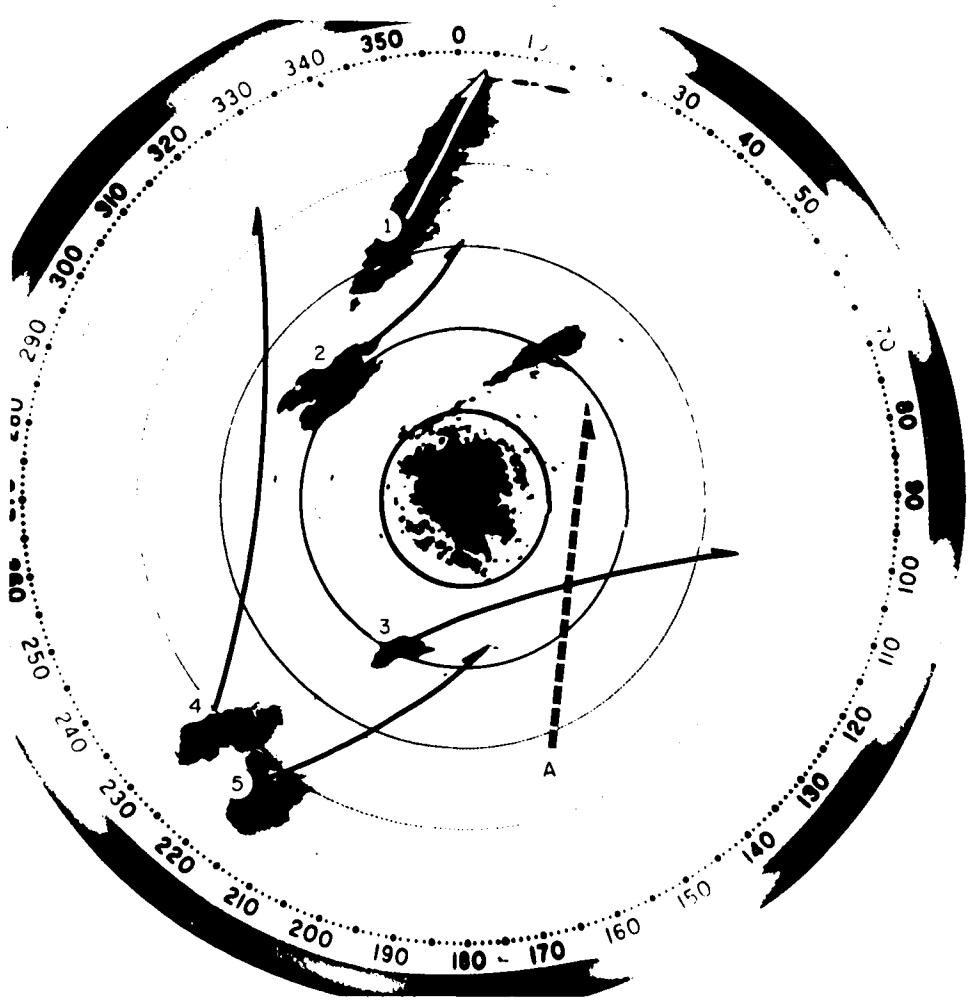

Figure 6. - WSR-57 radar PPI display and storm tracks, 100 n. mi. range, 20 n. mi. range marks, 1454 CST, April 3, 1964.

shows six thunderstorm areas early on the afternoon of April 3. Five of the storms are numbered for reference in individual motion calculations. The arrows show the approximate tracks of these storms. The sixth (unnumbered) soon dissipated without producing severe weather. The broken arrow shows the track of a shower which developed later at point "A" and moved northward to intercept echo No. 3. Figure 7 shows the corresponding display of the echo intensity integers. The digits represent 6-decibel increments of received power normalized to 100 n. mi. The integer "1" indicates a radar reflectivity factor of approximately 5 $mm.^{6} m.^{-3}$, and "7" indicates 1.9×10^{4} $mm.^{6} m.^{-3}$

The general motion of the composite echo is objectively defined in terms of correlation fields based on matching integers at addresses bearing a fixed spatial correspondence to one another in arrays separated in time. The location of the maximum correlation coefficient measures pattern displacement and its magnitude measures pattern development.

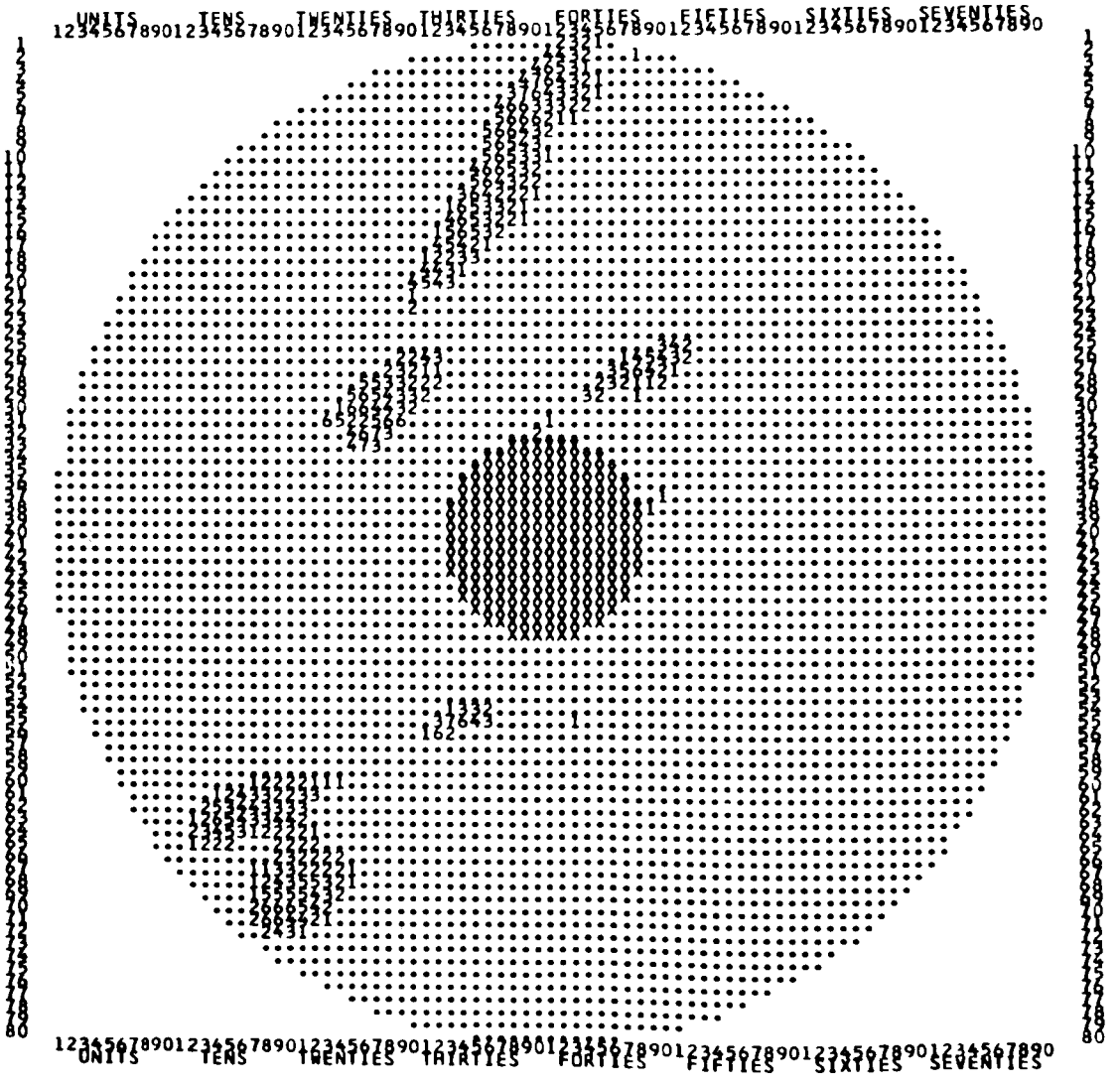

Figure 7. - Compilation of maximum echo intensity integers, 1454 CST, April 3, 1964.

The "zero" intensities, or no-echo points, are included in the correlation computation. The space-lag components I, J, associated with the maximum correlation coefficient, are related to echo velocity by:

$$V = \frac{2.5}{\tau} (I^2 + J^2)^{1/2} \qquad (1)$$

where τ is the time interval between arrays and the grid spacing is 2.5 n. mi.

J LAG / I LAG	-1	0	1	2	3
-4	0.34	0.49	0.59	0.62	0.58
-3	0.47	0.63	0.71	0.70	0.63
-2	0.57	0.69	0.73	0.67	0.57
-1	0.58	0.64	0.61	0.54	0.45
0	0.50	0.50	0.46	0.41	0.35

COMPOSITE ECHO

J LAG / I LAG	-2	-1	0	1	2
-3	0.00	-0.00	0.07	0.26	0.45
-2	0.13	0.26	0.48	0.76	0.70
-1	0.25	0.45	0.62	0.51	0.28
0	0.21	0.27	0.20	0.08	0.02
1	0.05	0.04	0.01	-0.00	-0.00

ECHC # 3

J LAG / I LAG	-2	-1	0	1	2
-4	0.29	0.42	0.53	0.59	0.58
-3	0.51	0.70	0.80	0.81	0.73
-2	0.65	0.82	0.88	0.80	0.65
-1	0.62	0.66	0.64	0.53	0.42
0	0.41	0.38	0.33	0.28	0.21

ECHO # 4

J LAG / I LAG	1	2	3	4	5
-4	0.14	0.26	0.42	0.54	0.57
-3	0.33	0.52	0.74	0.83	0.74
-2	0.52	0.73	0.91	0.89	0.71
-1	0.52	0.66	0.68	0.56	0.43
0	0.38	0.40	0.35	0.27	0.19

ECHO # 5

Figure 8. - Fields of cross correlation coefficient for 20-min. time lag, April 3, 1964.

Figure 8 shows the fields of coefficients computed for integer displays compared at 20-min. intervals. The field in the upper left is derived from comparisons of the total echo display. The remaining three fields are for the individual echoes, Nos. 3, 4, and 5, respectively.

There are two noteworthy features in these correlation fields. First, the location (lag) of the maximum value varies from echo to echo. The composite echo and echo 3 show similar I and J displacements, i. e., 2 grid units north (-I) and I grid unit east (J). Echo 4 shows only a northerly displacement and echo 5 has an east-northeast displacement. Obviously, the motions of echoes 4 and 5 are at variance with the mean echo velocity.

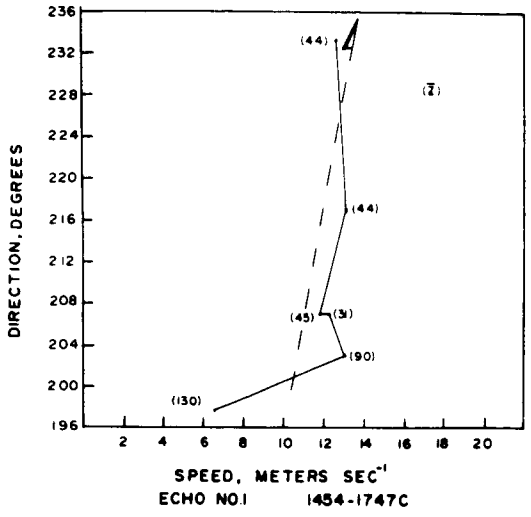

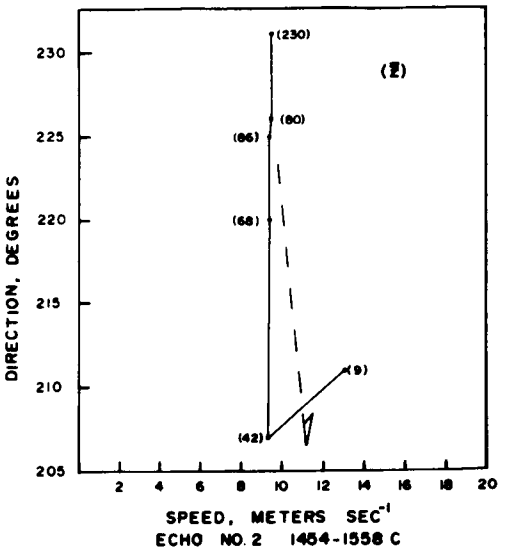

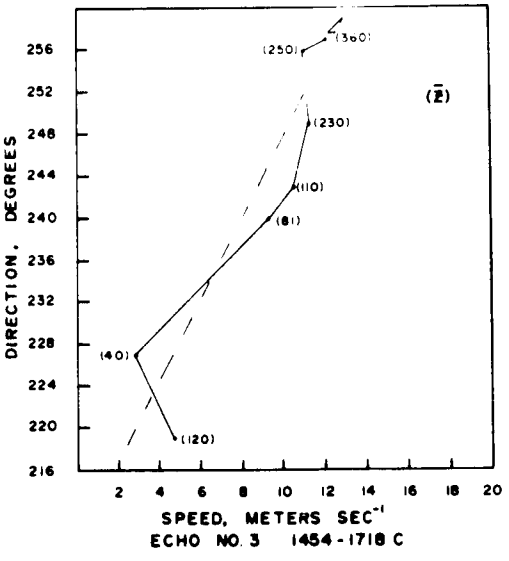

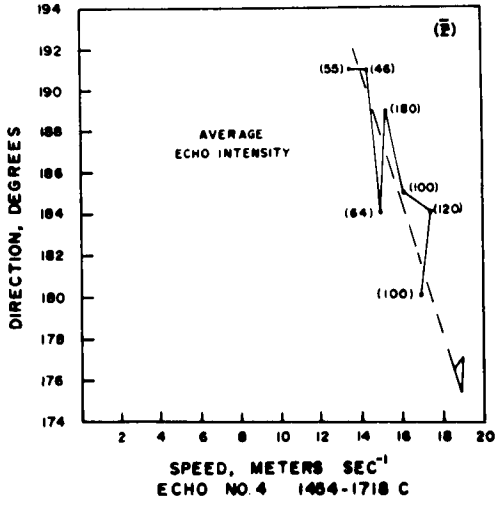

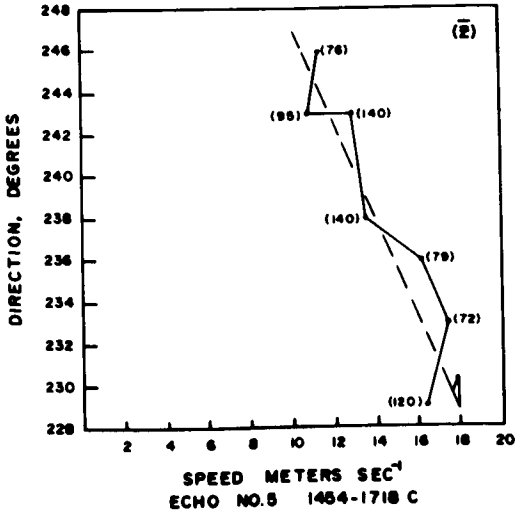

Figure 9. - Storm velocity profiles, April 3, 1964.

The second significant difference is in the magnitude of the correlation coefficients. Individual echoes 4 and 5 are relatively stable with values of 0.88 and 0.91. However, their divergent motions change the shape of the pattern containing several storms, and effectively lower the correlation coefficient for composite echo.

The five echoes persisted for 2 to 3 hours, an adequate period for determining average velocities. The time histories of the calculated velocities are shown in figure 9. The solid lines connect the point velocity measurements. The dashed line estimates the average change with the arrow indicating the direction of increasing time. The values in parentheses are arithmetic average Z values. Two of the storms (Nos. 1 and 3) veered with time; the remaining three storms backed with time.

The average rate of change in speed between 1500 and 1700 CST was approximately 4.5 m. sec.$^{-1}$ hr.$^{-1}$ This is about twice the change in mean layer wind speed as determined from radiosoundings at 0700 and 1600 CST at Fort Sill, Okla. The mean directions range from 238° (echo No. 3) to 186° (echo No. 4). The speeds range from approximately 10 to 15 m. sec.$^{-1}$ The overall average velocity is in good agreement with the 8-km mean layer wind of 225 deg., 13 m. sec.$^{-1}$ However, the range of the individual velocities is as great as the mean. The changes in intensity show no apparent relationship with the changes in velocity.

The large-scale analysis of the wind field may have smoothed out significant mesoscale disturbances. However, the 1600 and 1700 CST soundings made at Fort Sill should have detected a wind perturbation associated with the varying motions of storms 4 and 5. The algebraic average change between consecutive soundings indicates that the mean wind backed an average of 11 deg. during the hour. The average speed increased 4 m. sec.$^{-1}$, in close agreement with the acceleration of the echo field. Also, these two observations agree closely with the 0700 and 2000 CST soundings. Mesoscale analysis of the wind data does not show a basis for the great variability of individual storm motion.

4. IMPLICATIONS FOR SHORT-RANGE FORECASTS AND WARNINGS

The severe weather produced by the five storms is summarized in Table 1. A total of 83 observations of hail, damaging wind, heavy rain, and/or tornadoes was received from Volunteer Storm Observers. A vivid description of the very destructive tornado at Wichita Falls, Tex. (associated with echo No. 5 at 1506 CST) was documented by Stankewitz, et al [6].

The predicability of each of these five storms was evaluated by determining the number of pairs of matched intensity integers, i.e., a "1" on "1", "2" on "2", etc., for the optimum space lag defined by the maximum correlation coefficient. The displays were compared for four average time lags of 18, 34, 51, and 68 min. The total number of matched pairs of intensity values was converted to percent of total integers to provide the percent "hits" for each space extrapolation. The average maximum correlation coefficients and the average percent "hits" for all storms, and for each storm treated individually, are listed in Table 2. The last three columns in Table 2 show the average reflec-

TABLE I. - SEVERE WEATHER OBSERVATIONS

Storm No.	Hail	Wind	Tornado
1	max. 1/4 in. dia. (avg. 1/4)	no damage	none
2	max. 3 in. dia. (avg. 1 1/2)	no damage	none
3	max. 3 to 5 in. dia. (avg. 1/4 to 3/4)	damage to trees, property, and crops	tornado near Pauls Valley, Okla.
4	max. 2 to 3 in. dia. (avg. 1/2 to 3/4)	small amount to trees and crops	none none
5	max. 1 1/2 to 2 1/2 in. dia. (avg. 1/4 to 3/4)	trees and crops	tornado Wichita Falls, Tex. and Waurika, Okla.

tivity, maximum reflectivity, and equivalent water output rate for the storms.

The correlation coefficient is related to the per cent of hits. Wilson [5] has related the coefficient, the per cent of hits and the intensity variance for the relatively simple case where 0-0 pairs are excluded. Wilson shows that when the correlated patterns have the same average intensity and variance, the per cent hits increases with decreasing variance because of the predominance of a particular intensity integer.

The most important factor apparent in Table 2 is the relationship of maximum intensity to the predictability expressed by percent hits. For time lags of 51 and 68 min., the rankings of the two parameters are the same. (The ranking according to storm No. is 4, 3, 5, 2, and 1.) This increase in predictability with intensity is obviously important for forecasting severe weather events associated with existing thunderstorms.

The average intensity and water output are a function of total storm area and therefore not necessarily related to the maximum intensity.

5. COMMENTS ON THE VARIANCE OF STORM VELOCITIES

The two tornado-producing storms, Nos. 3 and 5, behaved as predicted from kinematic considerations developed by Newton and Fankhauser [7]. They have demonstrated that large storms migrate toward the direction of the low-level moisture. This

TABLE 2. - PREDICTABILITY OF INTENSITY INTEGERS APRIL 3, 1964.

	AVERAGE TIME LAG, MINUTES				AVG. INT.	MAX. INT.	WATER OUTPUT
	18	34	51	68	$mm^6 m^{-3}$	$mm^6 m^{-3} \times 10^4$	$m^3 hr^{-1} \times 10^6$
ALL STORMS							
Corre. Coeff.	0.67	0.68	0.61	0.57	76	130	12.3
Per Cent Hits	68%	59%	49%	41%			
STORM 1							
	0.65	0.42	0.25	0.14	64	3	2.7
	64%	41%	21%	12%			
STORM 2							
	0.67	0.64	0.60	0.58	86	9	1.6
	47%	44%	33%	21%			
STORM 3							
	0.83	0.75	0.70	0.60	170	34	3.8
	81%	76%	68%	50%			
STORM 4							
	0.78	0.73	0.71	0.72	95	130	2.3
	70%	70%	75%	77%			
STORM 5							
	0.86	0.86	0.83	0.82	103	9	1.9
	68%	66%	51%	47%			

would require the storms to deviate to the right of the mean environmental wind as observed. If the storms are rotating, the Magnus effect may contribute to this deviation, as suggested by Fujita [8], and modeled by Browning [9].

Echo No. 4 had the most exceptional motion. This storm moved northward, approximately 30 deg. to the left of the mean environmental wind. In order for the Magnus effect to result in this peculiar motion, the storm would have to be rotating anticyclonically.

Sasaki [10] has substantiated the association of particular surface pressure distributions around vortices (hurricanes) with particular storm motions. He has determined the effect on motion of an asymmetric inflow pattern resulting from a non-symmetric vortex. The model may steer the rotating severe storm to the right or left of the environmental wind. It is planned to examine the surface wind and pressure field in the vicinity of storm No. 4 to evaluate this model as well as possible rotational effects.

Batjer [11] suggests the anomalous motion can be attributed to areas of strong, warm advection below 500 meters. Such may have been the case on April 3, especially if the storm was tracing the motion of the interface between the low-level moisture and the cooler and drier air aloft.

The transport mechanism may be similar to the expansion wave described by Freeman [12]. A wave phenomenon seems applicable in a second example of northward propagation that occurred to the east of storm No. 3 between 1700 and 1800 CST. In this case, a convective shower, extending to 15,000 feet, moved northward through the leading edge and under the anvil of storm No. 3, and then continued northward for at least 20 n. mi. The lack of apparent modification of the shower by storm No. 3 suggests to the author that the shower was maintained and propagated northward by a wave in the low-level moisture field.

In addition to examining the individual echo velocities by objective techniques, a continuous motion study was made by constructing a 16 mm. movie from the original series of 35-mm. step-attenuation photographs. This movie permits one to view the relative motion of the storms at selected levels of intensity and at selected heights.

The motion study suggests that a wave may also have been influential in augmenting the vertical development of storm No. 3 at the time of the tornado occurrence near Pauls Valley, Okla.

The evidence of varied storm motion is clear. However, at present the cause (or causes) are mostly conjecture. Comprehensive observations of the three-dimensional environmental wind and storm structure may provide a basis for an empirical solution.

REFERENCES

1. Donaldson, R. V., Jr., "Radar Reflectivity Profiles in Thunderstorms," Journal of Meteorology, vol. 18, No. 3, 1961, pp. 292-305.

2. Wilk, K. E., "Radar Reflectivity Observations of Illinois Thunderstorms," Proceedings Ninth Weather Radar Conference, American Meteorological Society, Boston, 1961, pp. 127-132.

3. Ward, N.B., K. E. Wilk, and W. C. Herrmann, "WSR-57 Reflectivity Measurements and Hail Observations," NSSL Report No. 24, U. S. Weather Bureau, Aug. 1965.

4. Kessler, E., III and J. A. Russo, Jr., "Statistical Properties of Weather Radar Echoes," Proceedings 10th Weather Radar Conference, American Meteorological Society, Boston, 1963, pp. 25-33.

5. Wilson, James W., "Movement and Predictability of Radar Echoes," NSSL Report No. 28, ESSA, Aug. 1966.

6. Stankewitz, L. W., A. Johnson, and J. V. Dobry, "The Wichita Falls Tornado," Weatherwise, vol. 17, No. 2, Apr. 1964, p. 80.

7. Newton, Chester W., and James C. Fankhauser, "On the Movement of Convective Storms, with Emphais on Size Discrimination in Relation to Water Budget Requirements," Journal of Applied Meteorology, vol. 3, No. 6, 1964, pp. 651-668.

8. Fugita, T., "Proposed Mechanism of Hook Echo Formation," Research Paper No. 27, University of Chicago, National Severe Storm Project, U.S. Weather Bureau grant WBG-8, 1963.

9. Browning, K. A., and T. Fujita, "A Family Outbreak of Severe Local Storms - A Comprehensive Study of the Storms in Oklahoma on 26 May 1963, Part I," Special Reports, No. 32, Air Force Cambridge Research Laboratories, Bedford, Mass., Sept. 1965.

10. Sasaki, Y. and S. Syono, "Motion of the Vortex with Pressure and Inflow Which Are Not Circular Symmetry," University of Oklahoma, under research grant NSF GF-172, 1966.

11. Batjer, D., "Die Bemerkenswerte Gewitterlage vom 7. Juni 1964 über Norddeutschland," Meteorologische Rundschau, vol. 18, No. 1, Jg., Heft 1.

12. Freeman, J., "The Solution of Nonlinear Meteorological Problems by the Method of Characteristics," Compendum of Meteorology, American Meteorological Society, Boston, Mass., 1951, pp. 421-433.

AN ANALYSIS OF EIGHT FLIGHTS BY U-2 AIRCRAFT OVER SEVERE STORMS IN OKLAHOMA

WILLIAM T. ROACH

Meteorological Office
Bracknell, England

ABSTRACT

The method and results of the analysis of photographic records of the summit areas of severe storms obtained from a U-2 aircraft flying at an altitude of 65,000 ft. over Oklahoma are described.

Comparison of the heights of storm cells protruding through the main anvil cirrus deck of a squall line with the predictions of simple "parcel" theory suggests the latter may be used to indicate the maximum development attainable (but not necessarily attained) by a squall line on a given day.

It is suggested that temperatures approaching -100°C. may occur in the domes of giant quasi-steady storm cells reaching altitudes of 55,000 - 60,000 ft. Such a dome is probably bounded by a thin shell of extremely stable air, which is not inconsistent with the rather smooth texture of dome summits sometimes shown by the U-2 photographs.

1. INTRODUCTION

The U-2 is one of the few aircraft capable of flying over the giant convective (squall-line) storms which occur frequently in mid-western United States in late spring and early summer, and the photographic records present a potentially unique method of assessing the distribution of cloud and storm top heights in squall lines. Here are presented results of analysis of flight data and films obtained during eight flights by U.S. Air Force U-2 aircraft above Oklahoma storms.

Description of Flight Data

On each flight, cloud photographs were taken at intervals of 16 or 32 sec. on 70-mm. film with a panoramic camera having a field of view of about 180° x 45°. The film is moved past a fixed slot in synchronism with a rotating prism to give a 180° presentation perpendicular to the line of flight. A description of the construction and operation of the camera is obtainable

from the manufacturers (Perkins-Elmer Corporation), and some applications of its use in photogrammetry from U-2 aircraft have been published, e.g., Fitzgerald [2], Blackmer and Serebreny [1], Fujita, Styber, and Brown [6].

The aircraft was also instrumented to measure air temperature, wind (with Doppler navigation equipment), ozone concentration (a Regener photoluminescent instrument), the effective radiative temperature of the ground or cloud surface directly beneath the aircraft (a Barnes infrared radiometer), and electric field (sensors above and below the aircraft).

The data from all these instruments in addition to the standard aircraft data (position, airspeed, pressure, altitude, and heading) were tabulated at intervals of 5 sec. in a data log book accompanying the films.

The aircraft usually maintained a (pressure) altitude near 65,000 ft. while flying over the storm areas.

2. METHOD OF ANALYSIS

The main aim of the analysis was to obtain a general picture of the distribution and heights of cirrus and storm tops in squall-line storms and, where possible, rates of growth of storm tops and of the location of individual cells.

A search was then made for significant correlations between the distribution so obtained and other meteorological parameters derived from aircraft measurements and conventional upper air data.

Analysis of Photographs

The basis of the method of determining cloud top heights and positions was to measure the parallax displacement of a feature identifiable on two or more consecutive photographs and thus to derive the distance of the feature from the aircraft. The feature could then be plotted on a map showing the aircraft track and the positions at which photographs were taken.

Since most of the cloud tops protruded above a continuous sheet of cirrus, it was not possible to measure their vertical depth directly, but displacement of the tops below the artificial[1] horizon could be measured. This necessitated a careful fix of the horizon. The methods of film calibration and measurement are outlined in Appendix I.

---

[1]Corresponding to zenith angle of 90°

The height of the cirrus deck could not be measured directly because of the lack of identifiable features, but a reasonable estimate could be made in the vicinity of storm tops by measuring their protrusion from the cirrus deck. Then, knowing the height of the cirrus deck, a reasonable estimate of the location of the edges of the deck could be made (providing these were within about 60 n. mi. by using rectification scales provided by NSSL for the analysis of U-2 films.

The large time interval between frames made it impossible to measure the distance and, therefore, the height of features less than about 7 n. mi. from the aircraft, because close features were never visible on two consecutive frames. Since the aircraft flew directly above several big storm tops, a considerable amount of valuable information was lost in this way.

Each flight spent about 2 hr. in the storm area during which period a given part of the storm was viewed a few times by the camera at irregular intervals from a few minutes up to half an hour. It was possible in a few cases to identify a given storm top for two or more appearances and to comment on its evolution.

Rates of growth of a few tops could be measured quite accurately (about $\pm$200 ft./min. at a distance of 10-20 n. mi.

3. RESULTS

Of the eight flights examined, five were well-developed squall lines, four of which contained clouds exceeding 50,000 ft. in height. On the other three flights, the storms exhibited no synoptic-scale organization, were rather small, and were probably of air-mass type.

The three squall lines of greatest development were found roughly parallel to the dry-line[2] and within about 40 n. mi. of it. One squall-line was found some 100 n. mi. to the east of the dry line.

The three air-mass type cases were all over 100 n. mi. east of the dry line, and consisted of small scattered storms not exceeding 40,000 ft. in height.

Thus the main interest of the paper lies in the study of the well-developed squall lines.

Figures 1 - 4 show maps of the cloud distribution observed during half-hour periods on three days.

---

[2] A quasi-permanent boundary between very dry desert air and damp air of Mexican Gulf origin running approximately N-S somewhere between 95° and 105° W. during this season.

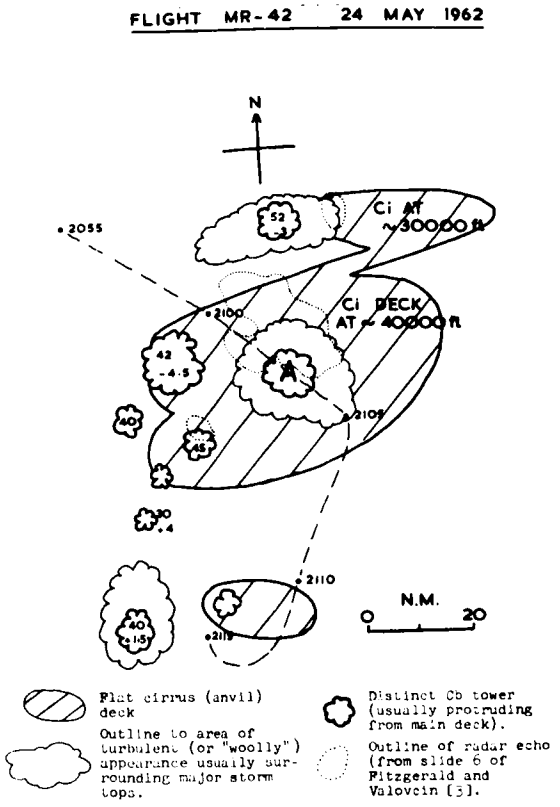

Figure 1. Cloud distribution observed at 2100 GMT May 24, 1962. Dashed line gives aircraft track with time (GMT) marked along it.

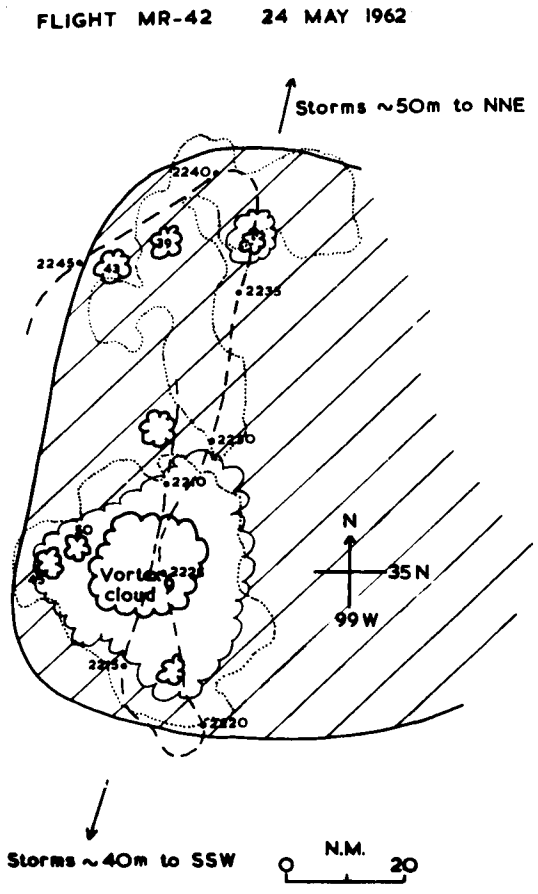

Figure 2. Cloud distribution observed at 2230 GMT May 24, 1962. Dashed line gives aircraft track with time (GMT) marked along it.
(See figure 1 for legend.)

General Features

Some features observed in major squall lines were as follows:

(i) The storm belts were generally oriented within 20° of a NNE-SSW direction.

(ii) The sheet of anvil cirrus generated by the storms spread out at a level near the equilibrium level predicted by "parcel" theory - usually somewhat above the environmental tropopause. The top of the cirrus deck thus produced a new tropopause.

(iii) The upstream (200-mb. wind) edge of the cirrus was well-defined, 70-200 n. mi. in length, and exhibited little movement during the flight period (about 2 hr.). The downstream edge was usually out of sight 100 n. mi. or more to the east.

(iv) On two flights, further storm areas or isolated storms were visible 50-100 n. mi. to the NNE and SSW of the limits of

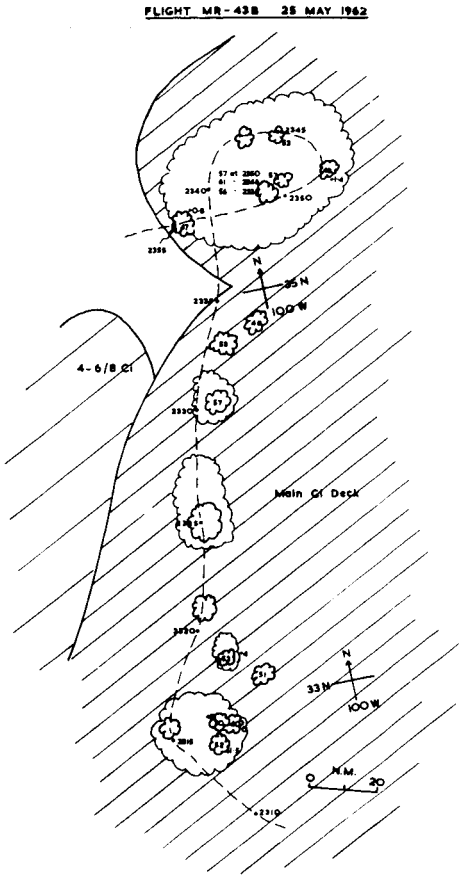

Figure 3. Cloud distribution observed at 2330 GMT May 25, 1962. Dashed line gives aircraft track with time (GMT) marked along it.
(See figure 1 for legend.)

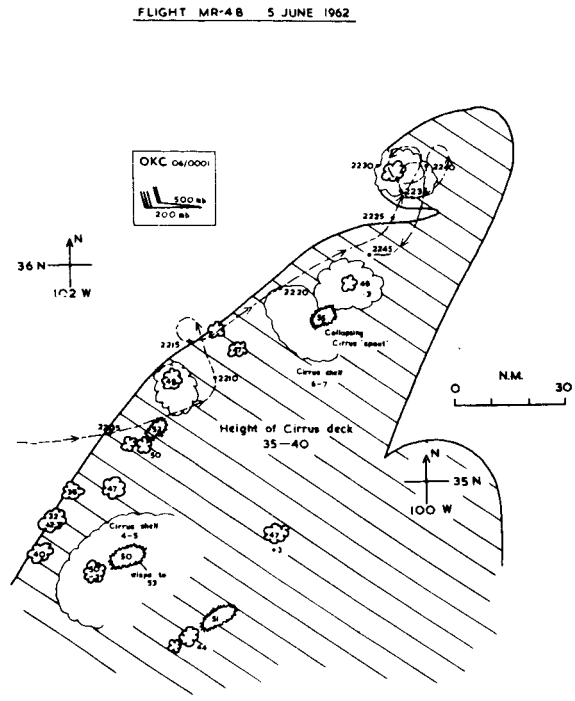

Figure 4. Cloud distribution observed at 2230 GMT June 5, 1962. Dashed line gives aircraft track with time (GMT) marked along it.
(See figure 1 for legend.)

the storm area under examination with their upstream edges apparently roughly aligned and probably lying along the same squall-line system.
(v) A storm top was typically 2-5 n. mi. in diameter (on one occasion as much as 7 n. mi.) and if protruding more than 6000-8000 ft. above the cirrus deck was usually surrounded by an area of cloud of violently turbulent appearance 10-40 n. mi. in diameter. The larger turbulent areas usually contained a few major storm tops and tapered from these down to the main cirrus deck in a rough cone with a slope of the order of 1 in 10.
(vi) Storm tops protruding through the cirrus sheet were mainly confined to a belt 20-40 n. mi. wide extending along the upstream edge of the cirrus with a density of about one top per 200-500 n. mi., i.e., about one top per 10-15 n. mi. along the length of the belt.

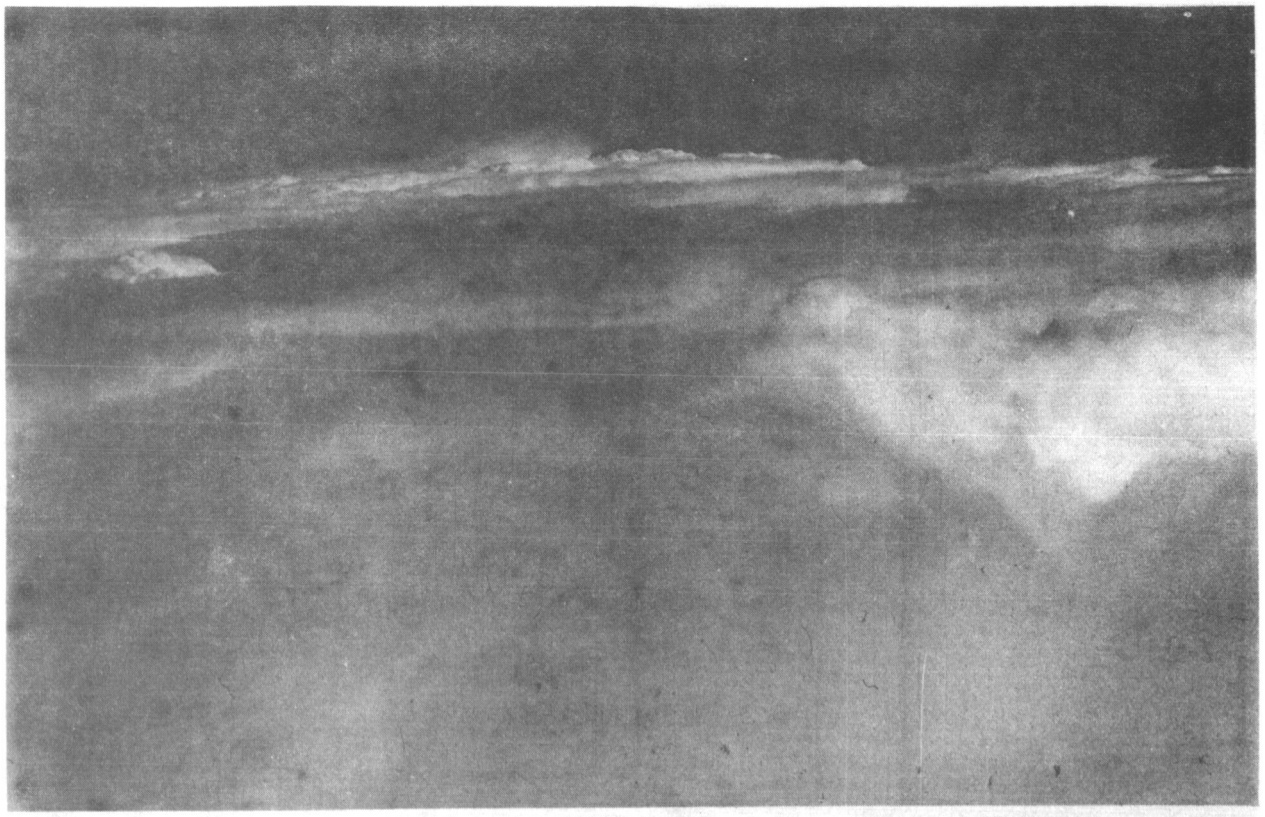

Figure 5. Small anvil formation above main cirrus anvil surface.

(vii) A subsiding storm top appeared to leave an area or dome of turbulent cloud with no well-defined top, but sometimes a separate small anvil of cirrus (fig. 5) 10-15 n. mi. long would form 10,000 ft. or more above the main sheet. These anvils are probably short lived (10-20 min.).
(viii) Rates of ascent and descent of a few individual tops up to about 5000 ft./min. were observed, but not exceeding about 2000 ft./min. for tops well above the environmental tropopause.
(ix) The distribution of storm height observed on a given flight was compared with the maximum height, Z_p, predicted by simple "parcel" theory, and it was found the highest tops slightly exceeded Z_p (probably not significant) on four flights while most of the tops were between 5000 and 10,000 ft. below Z_p. On the other four flights (which included one weak squall line) the highest tops observed fell 5000-15,000 ft. below Z_p.
(x) The highest storm top for which there is photographic evidence was 61,000 ft. (23,000 ft. above the environmental tropopause) with several tops between 55,000 and 60,000 ft. on that day. Wisps of cirrus were also observed at 63,000 ft.

Reports of tops of 60,000 ft. and more were found in pilot reports (based on visual estimates) on several days, including

days when photographic evidence suggested nothing above 50,000 ft.

It is suspected, however, that pilots judge top heights with respect to the visible horizon which at flight altitude is depressed 2-3° below the artificial horizon and would lead to an overestimate of top heights by 10,000 ft. or more. There is direct evidence of this in one case from 35-mm. photographs taken by the pilot of a distant top near the visible horizon reported as 64,000 ft. when, in fact, photogrammetric measurement put it at 50,000 ft. Thus, unless the pilot flies through or over a top within about 2000 ft., his visual estimates of cloud height are likely to be unreliable.

On Rates of Growth

It was observed that while instantaneous growth rates of individual Cb towers approaching 5000 ft./min. were observed (i.e., from growth over a period of 16 or 32 sec.), the growth rates observed for the few cells identifiable after a period of several minutes were an order of magnitude less.

This appears to be due to the fact that the "lifetime" of an individual tower (the time for which it has a visible identity) is generally less than 5 min. Each tower as it subsides is replaced (or displaced) by another tower which reaches approximately the same height as its predecessor. Thus the height of a storm cell above the tropopause probably changes at characteristic rates of a few hundred feet per minute, although there may well be exceptions in some cases.

Saunders [8] in an observational and theoretical study of the penetration of stable layers by cumulonimbus towers found the growth rate of a tower across the tropopause to be about 10 m./sec. for every kilometer of ultimate penetration, and above the tropopause to be approximately sinusoidal with a period of 3-4 min.

These empirical facts can be combined to give an expression of the form

$$P^2 = Z^2 + (W/\Omega)^2 \qquad (1)$$

where Z = observed height of tower above tropopause
W = observed rate of growth (or decline) of tower
$\Omega \simeq 0.6$ min.$^{-1}$
P = ultimate tropopause "penetration"

This expression is probably only applicable to the early growth stages of severe storms. Once developed, there is evidence that the height of a cell may maintain a constant altitude to within ± 5000 ft. for an hour or more.

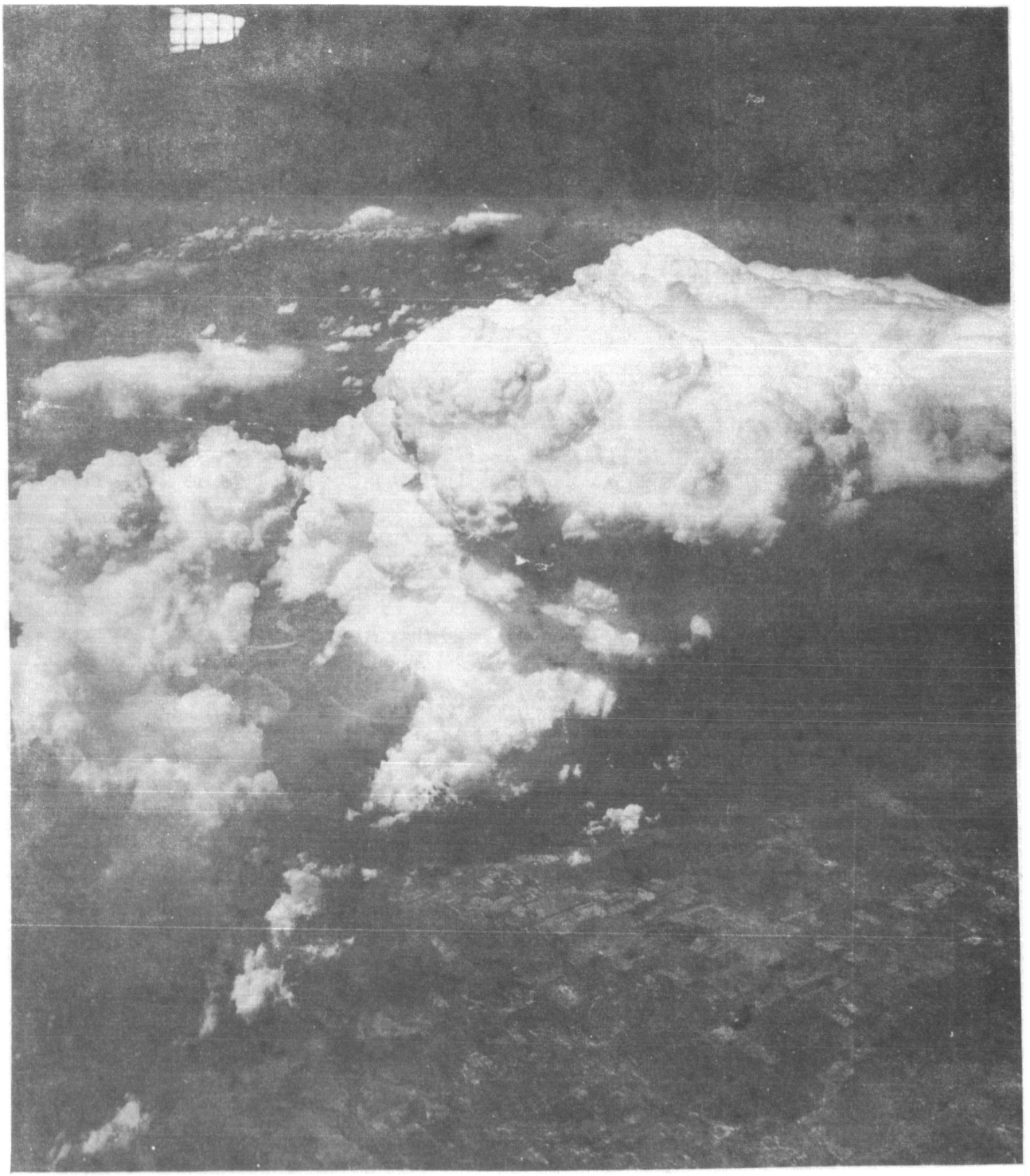

Figure 6. A line of developing severe storm cells.

Finally, there is reason to believe (see later discussion) that the rate of ascent in the updraught at the core of a growing or mature cell may approach its adiabatic value (from parcel method) which, at the tropopause, may be two to three times the rate of ascent of a growing tower (eq.1). There is also evidence of high vertical velocities from the existence of large hail and from aircraft penetrations of severe storms.

Features of Individual Storms

Flight MR-42: May 24, 1962

This storm is also discussed by Fujita [5] and Fitzgerald and Valovcin [3].

The aircraft arrived in the storm area during the early stages of development (fig. 1). A massive line of cells was seen to be developing (fig. 6) with hard cumuliform outlines. The leading cell was reaching 52,000 ft., and was producing a small radar echo at this time (2100 GMT). This cell was not identified on later traverses of this area.

Immediately afterward, the aircraft made its first pass over a large storm top (A, fig 1) surrounded by a disturbed area protruding from a cirrus deck being generated by this and smaller cells to the west. At this stage, the cirrus deck was a little over 50 n. mi. in diameter.

On subsequent passes, the area A was seen to increase in size steadily to about 40 n. mi. in diameter, and contained towers up to 57,000 ft. On the final pass at 2225 GMT (fig. 2), a curious formation was photographed (fig. 7) which has given rise to much discussion. Fitzgerald and Valovcin [3] interpreted the closely packed corrugation above the center of figure 7 as being the walls of a vortex circulation. This feature is discussed in Appendix II.

The center of the main cell moved northeastward at about 10 kt. during the flight period. No other cells were identifiable through more than one pass, although the cirrus sheet (and radar echo) developed toward the northeast and eventually measured 80-90 n. mi. along its upstream edge. This edge backed (in orientation) through about 30° during the flight period.

Further storm areas were visible some 50 n. mi. to the northeast and southwest of the boundaries of the storm area and were roughly aligned with it - probably along the same squall line.

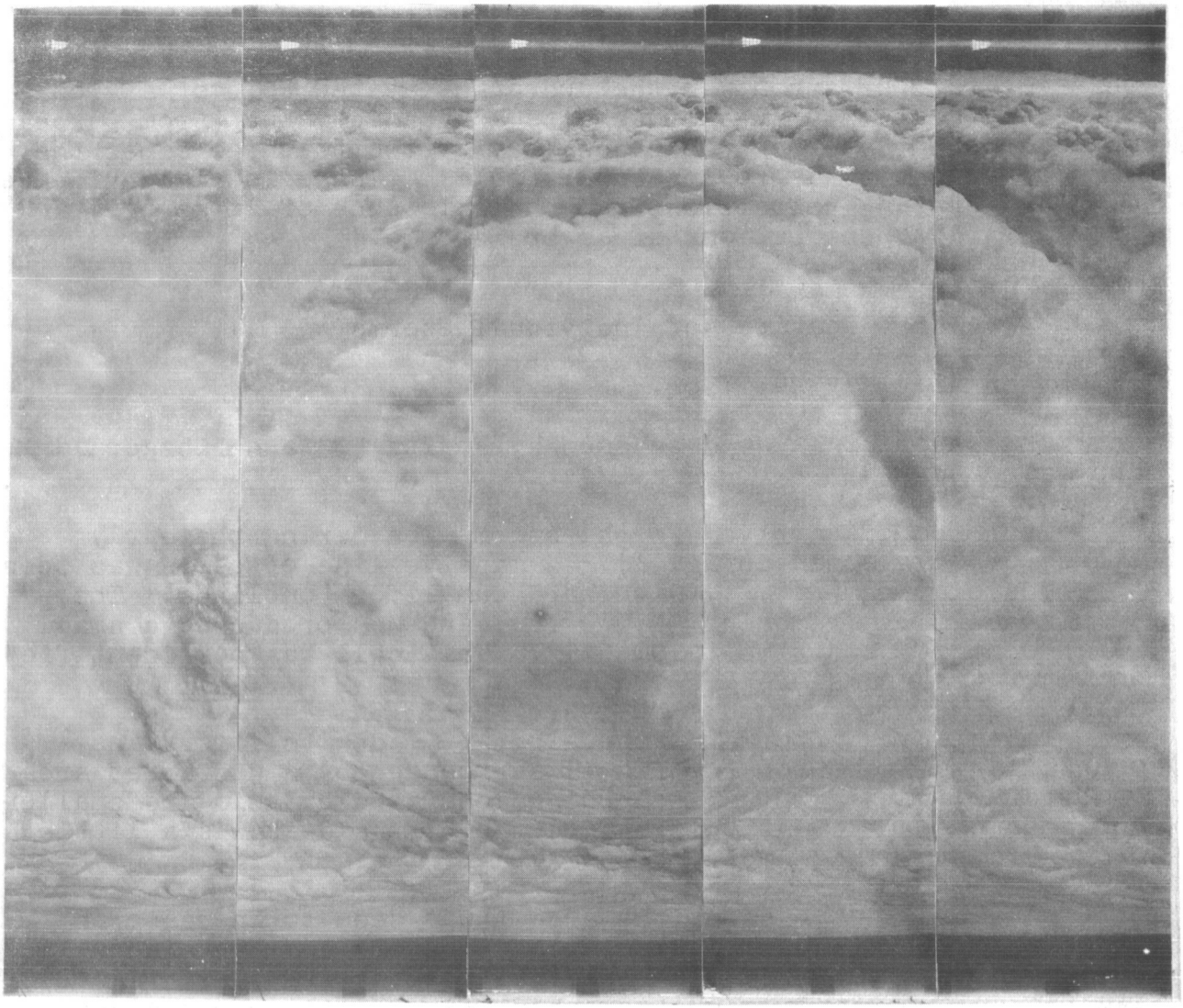

Figure 7. A mosaic of five consecutive frames taken at intervals of 32 sec. over a major storm top observed at 2225 GMT, May 24, 1962. (See also fig. 10, p. 40.)

Flight MR-43B: May 25, 1962

This was the day of greatest storm development of the series discussed in this paper.

Whereas the activity of the previous day was mainly concentrated in one great cell, the storms on this day were strung out in a band (fig. 3) connecting two great cells about 170 n. mi. apart in which the biggest towers were just exceeding 60,000 ft. Most of the storms between these cells exceeded 50,000 ft. in height.

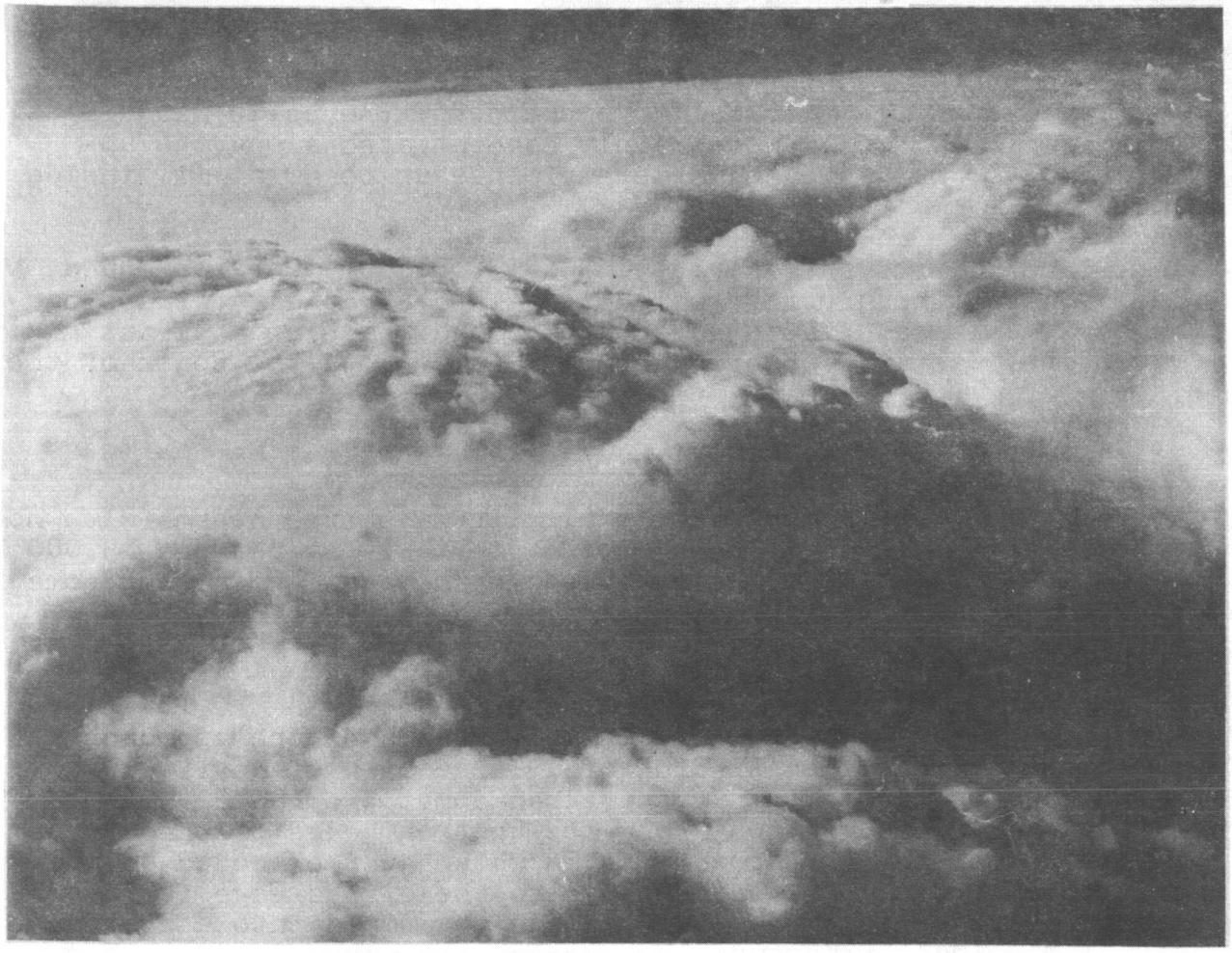

Figure 8. Major storm top observed at 2350 GMT on May 25, 1962.

The maximum parcel height of 58,000 ft. (R/S OKC, 0001 GMT May 26) was slightly exceeded by a few cells.

Figure 8 shows the main dome in the northern major cell, apparently in a quasi-steady state (not much height variation over several minutes). Its surface is relatively smooth compared to the area of violently turbulent cloud surrounding the dome. The visible base of the dome is 5-6 n. mi. in diameter and appears to form a distinct trench with the surrounding turbulent cloud.

Flight MR-45B: May 31, 1962

This was a day of restricted development with the aircraft flying along a squall line of small cells with tops in the range 30,000-40,000 ft. - well below the parcel height of 47,000 ft.

Flight MR-48: June 5, 1962

The storm area on this flight was as extensive as on May 25, 1962, although the vertical development of the cells was slightly less (fig. 4). Cells were mainly concentrated along the upstream edge, but some cells were visible up to 50 n. mi. inside the edge.

Three cirrus anvils (at 50,000-55,000 ft.) were observed, one close to the aircraft which contained a rapidly collapsing "spout". A great flattened dome of cloud reaching at least 55,000 ft. was also observed about 70 n. mi. to the south of the aircraft.

Flights EM-06, 07, 10: May 16, May 24, June 1, 1963

These appeared to be all small air-mass type storms with no obvious organisation. Their vertical extent lay between 25,000 and 35,000 ft. - the highest tops on each occasion falling some 15,000 ft. below the parcel theory height.

Flight EM-09: May 31, 1963

The aircraft passed some isolated cells on the approach to the main storm area consisting of a large area of anvil cirrus through which rather thinly scattered domes protruded, with an ill-defined concentration along the upstream edge of the cirrus. The major cell was a tornadic storm which just exceeded 50,000 ft. in height, and was near enough to the cirrus edge for the observers to see the low-level clouds organized into a distinct circulation pattern around the base of the storm.

Isolated storms (fig. 9) were visible 100-200 n. mi. to the SSW of the area and may have been part of the same squall-line system.

During the flight period, cirrus sheets produced by the isolated storms to the west of the main storm area grew, combined into one sheet, and spread toward the upstream edge of the main storm area, finally leaving a gap 10-15 n. mi. wide.

Distribution of Heights of Storm Tops

In table 1 is listed the distribution of storm top heights observed on the four flights over well-developed squall lines. The sample in all cases consists only of identifiable tops protruding above the main cirrus deck. In areas of major cells - consisting of a violently disturbed area up to 40 n. mi. in diameter - it was usually possible to pick out one to four major tops which were included in the sample. No attempt was made to

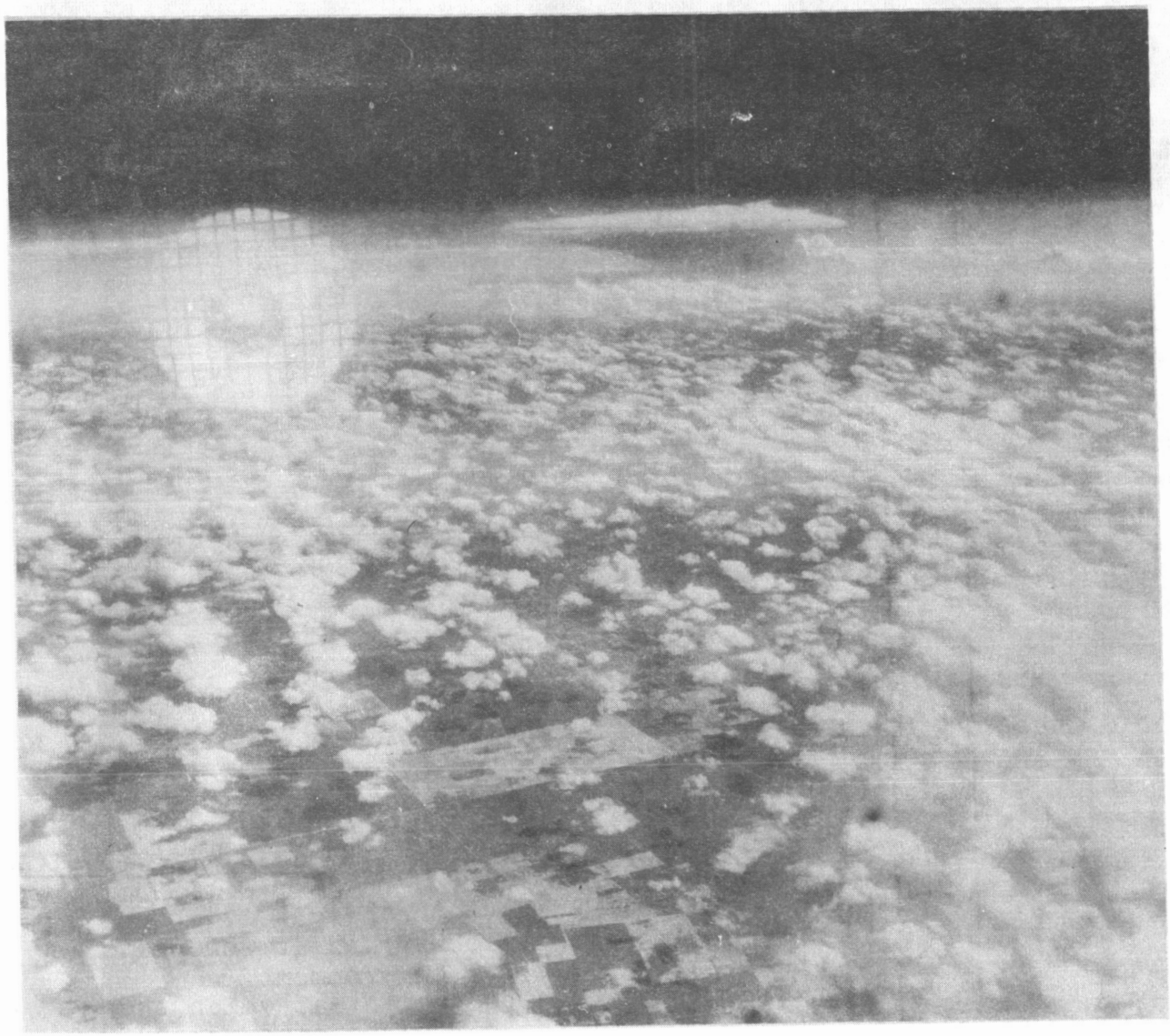

Figure 9. An isolated storm 120 n. mi. to the south of the aircraft observed on May 31, 1963. An aircraft horizon marker appears at top left (not used in analysis).

analyze these turbulent areas in detail or to pick out summits not clearly above the general level of the turbulent areas.

All heights are effectively pressure altitude - being measured relative to the aircraft pressure altitude, itself about 1000 ft. below its true altitude. The errors in the aircraft altimeter are not known, and it is assumed these have already been allowed for in the data log.

Table 1. Observed heights of storm tops

Ht. band (K ft)	Flight No. MR-42	MR-43B	MR-48	EM-09
37-39	1	0	1	0
40-42	6	2	1	3
43-45	2	2	2	5
46-48	2	2	7	0
49-41	3	2	6	5
52-54	2	3	2	0
55-57	1	3	2	0
58-60	0	2	0	0
61+	0	1	0	0
Mean ($\bar{Z}_s$)	46.0	51.2	48.5	44.2
σ	5.5	6.5	5.2	5.3
Z_e	40.4	42.2	43.0	38.6
Z_p	53.3	57.5	55.2	48.3
Highest top $(Z_s)max$	57	61	55-60	51
Z_T	38	38	42	37
Cī deck	40	42	44	42
Areal concentration of tops (1 per N sq. mi.) N	450	490	400	650

Z_e = Equilibrium parcel height - the height at which parcel reaches maximum velocity and at which its temperature is equal to its environment.

Z_p = Maximum parcel height - the height at which the vertical velocity of the parcel becomes zero due to increasing negative buoyancy; the height at which negative area is equal to the positive area on a thermodynamic diagram.

Z_T = Height of tropopause

$\bar{Z}_s$ = Mean storm top height

σ = Standard deviation of values of Z_s observed on one day

The height of the main cirrus deck appeared to lie somewhere near the equilibrium parcel level, Z_e, i.e., slightly above the level of the environmental tropopause, but the top of the cirrus deck appeared to slope down toward its upstream edge by 5000 ft. or more.

Forecasting Aspects

Examination of table 1 reveals a fairly consistent relationship between the mean height, $\bar{Z}_s$ reached by the tops, the maximum height reached, (Z_s) max, and the maximum parcel height Z_p. In particular, we note that $Z_p - (Z_s)\ \text{max} \sim 2000$ ft.

There is evidence from cumulonimbus height top observations from various parts of the world (Roach - to be published) that the parameter Z_p appears to be a useful predictor of the maximum height reached by Cb over a range of 20,000 ft.

Thus the forecasting problem can be defined as
(i) Forecasting ascent (environment) curve and maximum diurnal wet bulb potential temperature of air in lowest 100-150 mb.
(ii) Deciding whether other synoptic features present will trigger off thunderstorms.

It follows that Z_p predicts only the worst possible conditions, but says nothing, by itself, of the extent to which convection will develop.

However, we may use the relationship between Z_p and other parameters to say something about the worst conditions likely to develop on a given day.

For severe storms over Oklahoma it would appear that

$$Z_p - \bar{Z}_s \sim 7000 \text{ ft}$$
$$\sigma(Z_s) \sim 5500 \text{ ft}$$

We may now use these figures together with the storm top density (about 1 per 500 n. mi.^{2}) to form table 2 of the number of tops exceeding 50,000, 55,000 or 60,000 ft. likely to occur per 100 n. mi. along a squall line as a function of Z_p.

We assume a Gaussian distribution, and that the tops are confined within a belt 30 n. mi. in width along the upstream edge of the main cirrus deck.

Table 2. Number of tops exceeding 50,000, 55,000 or 60,000 ft. likely to occur per 100 n. mi. as a function of Z_p.

Z_p (ft.)	$Z_s \geq$ 50,000	55,000	60,000
45,000	0.1		
50,000	0.5	0.1	
55,000	2	0.5	0.1
60,000	5	2	0.5

Thus the risk of encounter with a Cb top at a flight level [illegible],000 ft. probably becomes serious for Z_p > 55,000 ft. This does not, of course, take into account the fact that associated turbulence may be found up to at least 5000 ft. above visible storm tops.

It must also be emphasized that this table is based on very few observations, applies only to severe storms in the Mid-West United States, and is intended to forecast the worst (and not necessarily the actual) conditions likely to be associated with a given unstable forecast ascent.

Correlation With Other Parameters

Temperature

There were three air temperature recorders used on the U-2 aircraft. Two of these showed good agreement with each other but, unfortunately, their short-period fluctuations in temperature were highly negatively correlated with fluctuations in airspeed, suggesting the correction for kinetic heating was too large. The third instrument was reading about 7°C. too high, but its fluctuations were uncorrelated with airspeed fluctuations, and not very well correlated with fluctuations of the first two instruments. Thus the interpretation of individual fluctuations was so uncertain that it was not possible to attempt a useful correlation with cloud distribution.

However, it is clear that temperature fluctuations as a whole increased markedly over storm areas - covering a range of up to 5°C. (as compared to 1°-2°C. away from storm areas) and there is some evidence that changes of 3°-4°C. in 5-10 n. mi. occur occasionally at 65,000 ft.

Radiometer

A radiometer designed to measure radiation in the spectral band 7.5-13μ and having a field of view of 2^{o} x 2^{o} was mounted to look straight down beneath the aircraft. Thus its resolution on a cloud surface 10,000 ft. below the aircraft was about 350 ft.

The results obtained on some of these flights have been already discussed by Fitzgerald and Valovcin [3], who found the effective radiation temperature of the cloud surface of a major dome to have a distinctive pattern, with a temperature minimum near the dome center, increasing to a maximum in the "trench" often observed around the base of the dome (or where the dome disappears under surrounding cloud). This is shown in the radiometer trace in figure 10 reproduced from Fitzgerald and Valovcin's paper. The level of temperature of these dome surfaces is of some interest - only dropping some 5^{o}-10^{o}C. below the surface of the surrounding cloud and cirrus deck.

Away from these domes, the radiometer temperature fluctuated considerably, even over an apparently flat cirrus deck.

Wind Field

The wind vector at aircraft levels (measured by the Doppler navigational system) appeared to be fairly steady away from the storm area, but exhibited large fluctuations while over the storm area. No systematic pattern could be discerned in this area, and it has been pointed out by Fujita [4] that the "wet beam" effect - i.e., one beam of the Doppler radar may be looking at heavy precipitation and not at the ground - may produce substantial errors in the wind vector. Therefore, analysis of the wind observations over the storm areas has not been attempted.

Ozone Concentration

Fluctuations in ozone concentration appeared to be mainly correlated with fluctuations in aircraft altitude. At a given level, fluctuations of $\pm$ 10-20% were observed, but showed no clear correlation with cloud distribution. There also appeared to be a distinct periodic fluctuation of the order of 3 min. which may have been instrumental in nature. The general level of ozone concentration was observed to be in the range 50-100 μg./m.^{3}(0.4 - 1.7 p.p.m. by volume) at 65,000 ft. on all flights.

Electrical Field

These observations have been discussed by Fitzgerald and Valovcin [3].

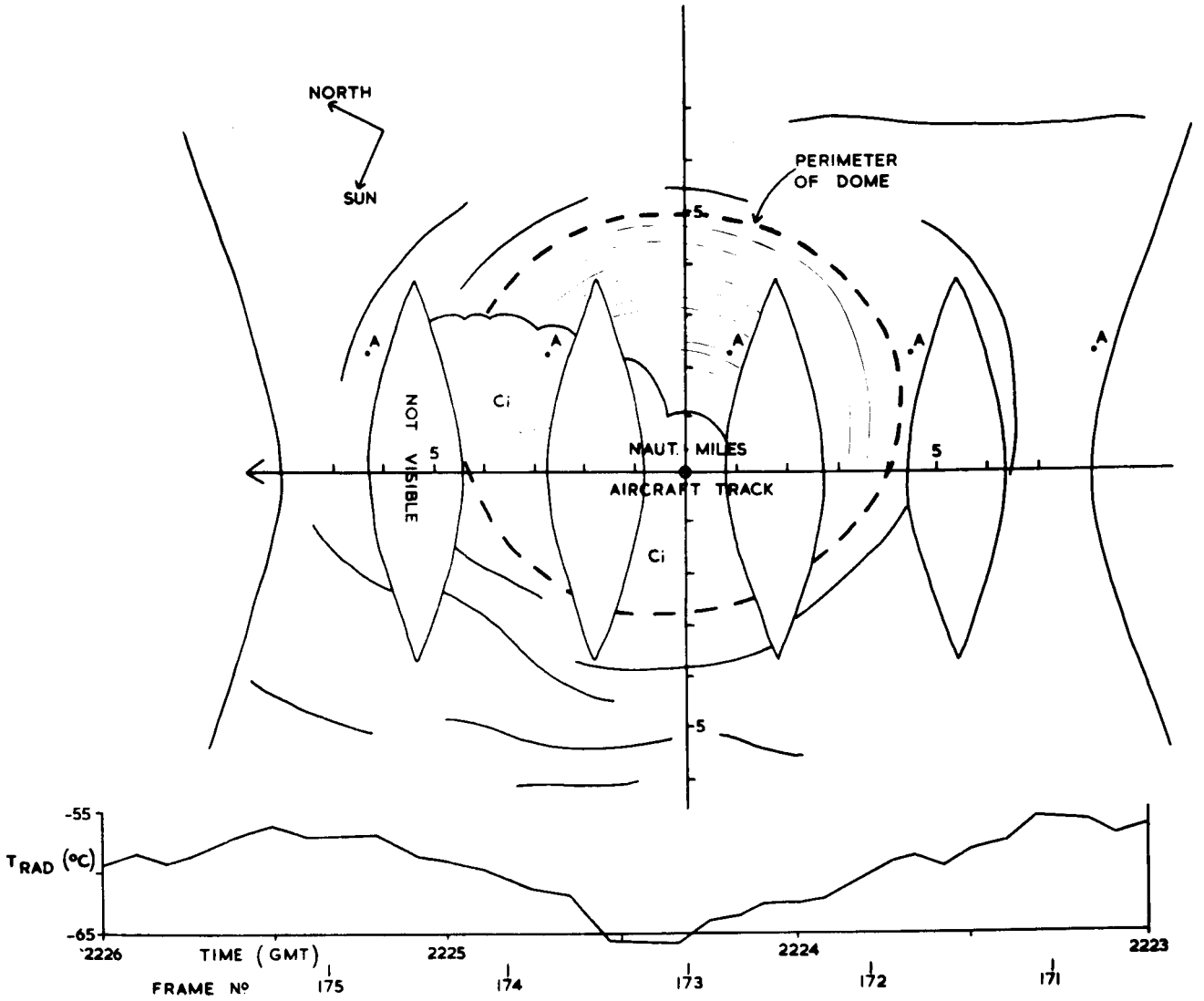

Figure 10. An attempted rectification of storm top shown in figure 7 onto a plane surface at 54,000 ft. altitude.' The thick lines outside the main dome show the approximate location of distinct cloud ridges. The trace at the bottom of the diagram represents the radiometer temperature of the dome immediately beneath the aircraft track (from [3]). (See discussion pp. 31 and 41.)

4. DISCUSSION

The main question on which a study of this kind might be expected to throw some light is: Is it possible to attempt the formulation of a model of the flow of air and hydrometeors through a storm top? Subsidiary questions of a more specific nature are:

(i) To what extent does simple parcel theory describe the behavior of the flow of air through a storm top and out into the main anvil?

(ii) How effective is the severe convective storm as a mechanism for the interchange of air between the stratosphere and troposhere? A related question is the mode of generation and dissipation of cirrus well above the main anvil cloud.
(iii) What evidence is there for rotation of the main updraught of a major storm cell?

Parcel Theory

Simple parcel theory predicts the variation with height of the vertical velocity and temperature of a buoyant parcel rising adiabatically and unmixed through a given environment. The parcel is assumed to lose its products of condensation (by fallout) while retaining the latent heat released. The equations of continuity and horizontal equations of motion are also neglected.

In cumulus convection, neglect of the mixing term renders parcel theory invalid. However, it was suggested by Ludlam [7] that since tops of severe storms are sometimes observed to reach the height predicted by parcel theory, and since the associated anvil cloud spreads out close to the parcel "equilibrium" level (parcel temperature equal to environment temperature) and presumably consists mainly of air expelled from the main updraught, this air may well follow closely the predictions of parcel theory. It would appear that the updraught is wide enough to prevent the mixing processes around its perimeter from penetrating to its core before this reaches the maximum parcel height, while the quasi-steady nature of the updraught may render aerodynamic drag negligible.

In figure 11 is shown the representative environmental and parcel ascent curves for Oklahoma City at 2100 GMT, May 25, 1962 (i.e., close to the time and area of flight MR-43B). This predicts a maximum vertical velocity of nearly 100 m. sec.$^{-1}$ at Z_e and a minimum temperature of -103°C. at Z_p. On this day, the highest top exceeded Z_p by about 3000 ft.

The dashed curve through the negative area shows an alternative path for ascending air suggested by Saunders [8]. He pointed out that if effective mixing of the updraught air with its environment sets in just above the tropopause, the dilution of negative buoyancy caused by mixing of updraught air with a relatively warm environment would roughly offset the effect of dilution of vertical updraught momentum. Then cloud air could approach Z_p without necessarily reaching the very low temperatures predicted by parcel theory. If this were the case, however, it might be expected the updraught air would subsequently follow a path similar to the straight dashed line in figure 11 and form an anvil cloud much farther above the tropopause than in fact is

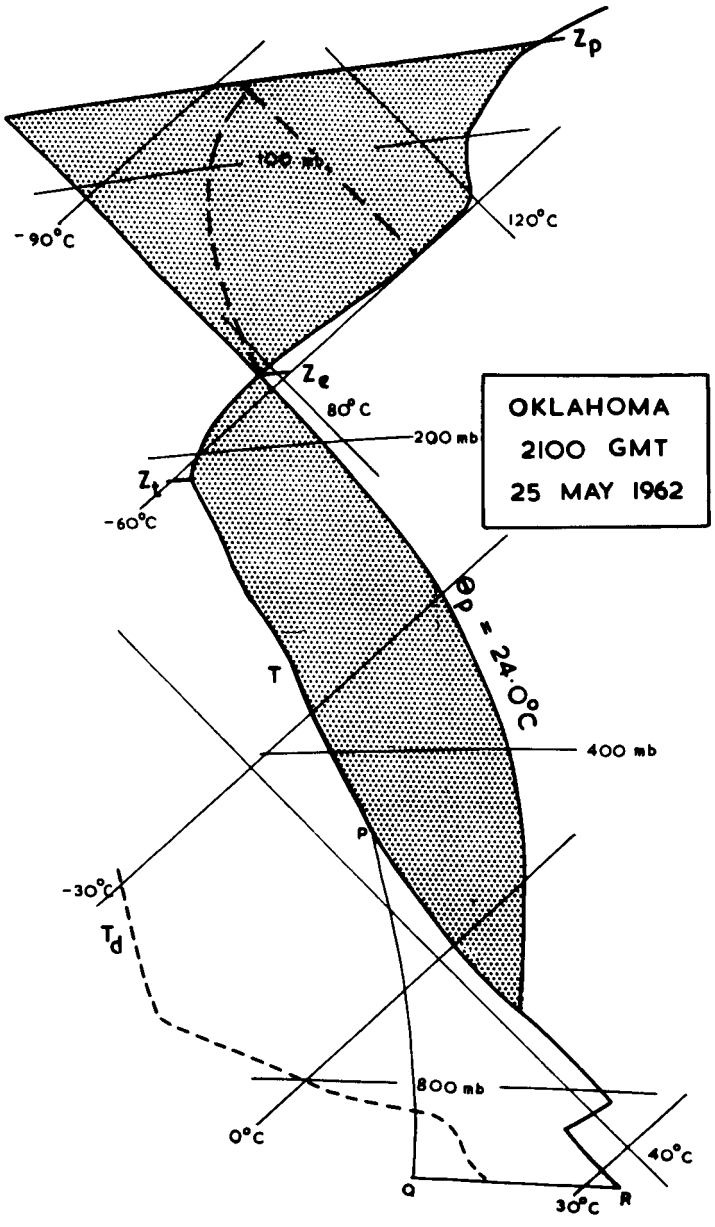

Figure 11. Representative environmental and parcel ascent curves for Oklahoma City 2100 GMT, May 25, 1962. Z_T = tropopause height; Z_e = equilibrium parcel height; Z_p = maximum parcel height.

observed[3] in severe storms. Saunders' analysis was intended to study tropopause penetration of growing air-mass storms and treated an ascending tower as a discrete entity of variable mass

---

[3]There is some evidence that air mass storms in United Kingdom form anvils between Z_e and Z_p, i.e., above the environmental tropopause.

(determined by the mixing process). However, the updraught in a severe storm often appears to attain a quasi-steady state with little variation in its general properties over a period long compared with the 5-10 min. it takes for air to pass through it. In this case the dynamical equations of a continuous fluid are probably more appropriate for analysis.

In regard to the updraught of a severe storm, it would seem reasonable to postulate that very low temperatures are indeed reached near the dome summit. This must be reconciled with radiometer observations that the radiative temperature of storm tops has never been observed to drop below about -70°C.

Model of a Storm Top

A tentative model of the distribution of flow and temperature in a storm top is shown in figure 12. This model postulates a dome of cold air supported by a quasi-steady updraught, and capped by a thin shell in which small-scale, intense mixing presumably takes place. Since this layer must be extremely stable,

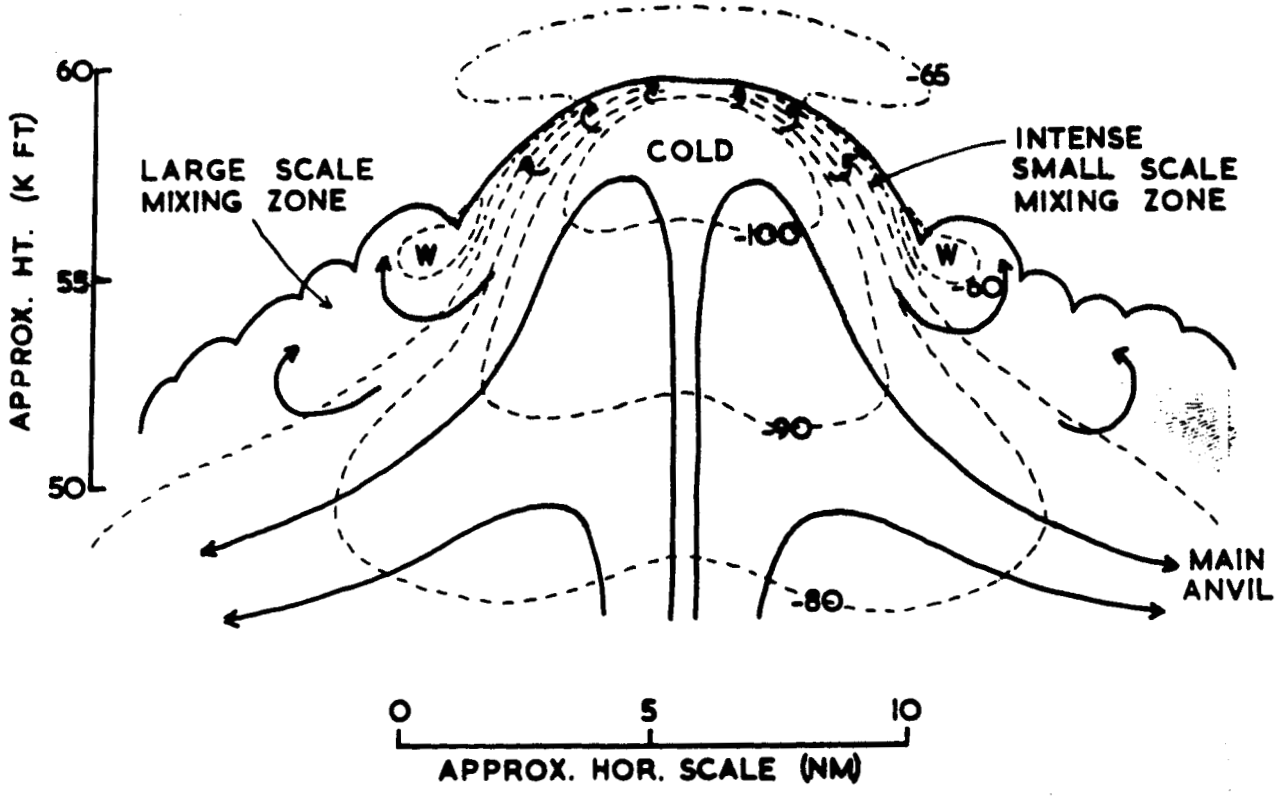

Figure 12. Tentative model of quasi-steady storm top. Dashed lines are isotherms (°C.); thin solid lines, the outline of clouds and streamlines of relative wind above the storm top; heavy solid lines, the streamlines of flow near center of updraught.

this mixing must be mechanically induced by strong local wind shear produced possibly by minor fluctuations in the updraught flux or lateral vacillations of the updraught axis near its summit. There may also be a relative motion of the dome with respect to the environmental wind field which could be anything up to 50 kt. and which may produce wind shear in the dome surface.

The appearance of the visible surface of storm tops protruding through the main anvil sheet is of interest. Usually, they have a similar appearance to the familiar cauliflower texture of growing cumulus, even though they must be entirely glaciated at these levels. However, some of the major domes exceeding 55,000 ft. in height observed on May 24 and 25, 1962, show a much smoother surface texture. The visible surface of the giant dome observed on May 24 (fig. 7) and discussed in Appendix II appears to consist of rather flat concentric ripples increasing in size from the center and suggesting a close approximation to the model (fig. 12). The dome observed on May 29 (fig. 8, p. 25) also possessed a fairly regular profile and radial surface markings. The diameter of the dome on May 24 was 7-8 n. mi. as compared to 5-6 n. mi. on May 25.

The comparatively smooth dome surface is in marked contrast to the turbulent sea of cloud in which it is embedded, and it cannot be ascertained to what extent this is due to mixing of the outflow of air in the main anvil with its stratospheric environment, or conflict between the outflow from adjacent domes. It is pointed out that horizontal velocities of the order of 100 kt. are probably reached in the main outflow 10-20 km. from an updraught center which will produce large local vertical wind shears.

Tropospheric - Stratospheric Interchange

The model postulated in the previous section suggests that most of the flux of air through the updraught settles out near the tropopause with negligible mixing with stratospheric air.

The most effective mixing phase probably occurs during the initial growth of the storm top into the stratosphere; this probably resembles the Saunders model discussed in the last section.

The air passing through the mixing zones in the cap of the dome and its surroundings will have acquired a higher potential temperature and must settle out at levels well above the main anvil. Since the air is cloud-free away from the main domes, there must be a flux of air through the visual cloud boundaries, and there is some evidence of this from the fragments of cirrus usually to be found hanging around the storm tops. It cannot be determined from the records available whether this cirrus evaporates, or falls back into the main cloud mass. If there is

evaporation, then this is a mechanism for introducing water vapor into mid-stratospheric levels, although in undetermined and probably negligible quantities.

ACKNOWLEDGMENTS

The author has benefited from discussions with Prof. Ludlam of Imperial College, Prof. Fujita of Chicago University, Mr. Harrold of the Meteorological Office, and scientists at Air Force Cambridge Research Laboratories, Bedford, Mass. and at NSSL, Norman, Oklahoma.

REFERENCES

1. Blackmer, R. H. and S. M. Serebreny, "Dimensions and Distributions of Cumulus Clouds As Shown by U-2 Photographs," Stanford Research Institute, Scientific Report No. 4 on Air Force Contract AF 19(604)-7312; Menlo Park, Calif., 1962.

2. Fitzgerald, D. R. "Nomogram for Analysis of 70-mm. Panoramic Camera Film," Unpublished Note, Air Force Cambridge Research Laboratories, 1962.

3. Fitzgerald, D. R. and F. R. Valovcin, "High Altitude Observations of the Development of a Tornado Producing Thunderstorm," Presentation at Conference on Physics and Dynamics of Cloud, Chicago, March 1964.

4. Fujita, T., "Accurate Calibration of Doppler Winds for Their Use in the Computation of Mesoscale Wind Fields," Monthly Weather Review, vol. 94, No. 1, January 1966, pp. 19-35.

5. Fujita, T., "Analysis of Selected Aircraft Data From NSSP, 1962," Dept. Geophysical Science, University of Chicago, Mesometeorology Project Research Paper No. 11, on Contract Cwb 10201, 1962.

6. Fujita, T., K. A. Styber, and R. A. Brown, "On the Mesometeorological Field Studies Near Flagstaff, Arizona," Journal of Applied Meteorology, vol 1, No. 1, March 1962, pp. 26-42.

7. Ludlam, F. H., "Severe Local Storms: A Review," American Meteorological Society, Meteorological Monographs, vol. 5, No. 27, 1963, pp. 1-28.

8. Saunders, P. M. "Penetrative Convection in Stably Stratified Fluids," Tellus, vol. 14, No. 2, May 1962, pp. 177-194.

APPENDIX I

Photogrammetry

The application of photogrammetry to the measurement of cloud top heights in this context does not appear to have been discussed before, so is described here in some detail.

The conversion from a measured distance, d, on a photographic plate to the angle, β, subtended by d is given by

$$\beta = d/F \qquad (1)$$

where F = focal length of camera.

If d is the parallax displacement of a feature between consecutive frames, (fig. 13), its distance, D, from the aircraft is given approximately by

$$D = Vt\ F/d = Vt/\beta \qquad (2)$$

where V = speed of aircraft relative to feature
t = time between consecutive frames.

In practice, accurate photogrammetry is only possible if the ground is visible, when accurate fixes can be made. In the application here, the aircraft spent long periods over continuous cloud, and most of the measurements were made on cloud tops within 15° of the horizon and of the direction perpendicular to the aircraft heading, hence cosine effects were neglected and V was taken to be the true air speed of the aircraft. The effect of yaw can be minimized by observing d for more than two frames whenever possible.

When the distances of the cloud top under examination are determined, it is then necessary to measure its height relative to the aircraft by measuring its displacement, Z (fig. 13) below the artificial horizon - some 2°-3° above the visible horizon.

The basic geometry of the problem is illustrated in figure 14. h is the aircraft altitude and h_c the altitude of the cloud top, D its distance from the aircraft, and R the earth's radius, α is the observed angular depression of C below the artificial horizon AA'. We have

$$\frac{R + h_c}{\cos \alpha} = \frac{D}{\sin \theta} = \frac{h + R}{\cos(\alpha - \theta)}$$

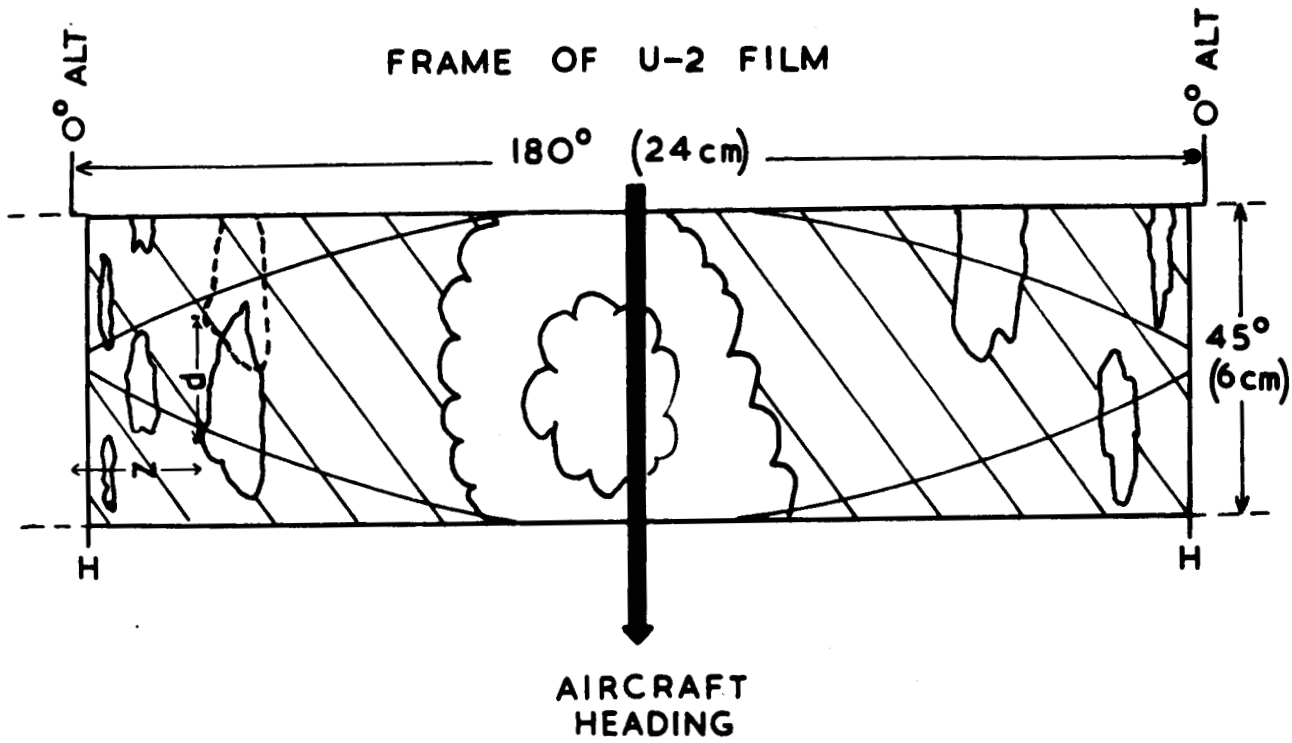

Figure 13. Format of one frame of 70-mm. film.

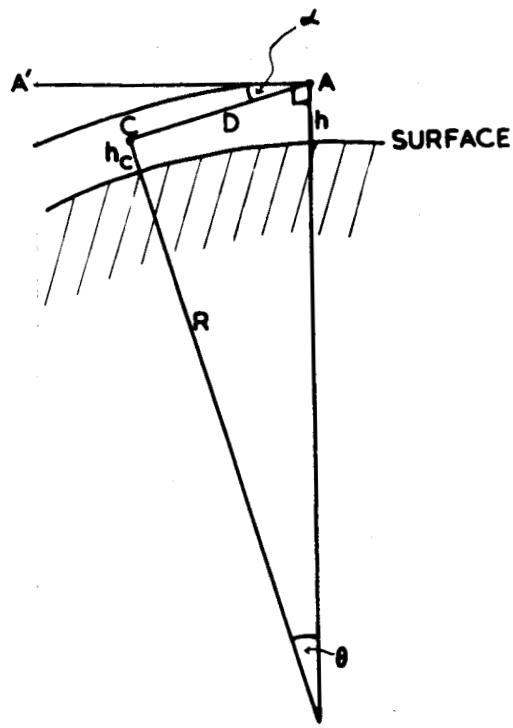

Figure 14. Geometry of cloud top height measurement from an aircraft.

Since α and θ are small, the trigonometric expressions can be expanded as the first term of their series, and assuming that $D = R\theta$, we obtain

$$h - h_c = D(\alpha - \frac{D}{2R}) \qquad (3)$$

where the second term on the right hand side is simply a correction for earth curvature, and is negligible for D < about 30 n. mi.

In order to determine h_c, however, α has to be measured, and this necessitates the determination of the exact position of the artificial horizons on the photograph (fig. 5). If the focal length of the camera is known, then the artificial horizon can be fixed by placing the visible horizon (HH in fig. 13) symmetrically between the artificial horizons

(whose separation is known). However, a difficulty arises here since it appears from a consideration of the errors in the terms in eq. (3), the focal length of the camera has to be known to within about 1/2 percent in order not to contribute an error at least as large as other errors incurred by the assumptions made in the main analysis.

The focal length of the camera is quoted as 3 in. (7.62 cm.) but it was possible to obtain an independent check on this as follows: Figure 9 shows an isolated storm at a distance of about 120 n. mi. from the aircraft. At this distance, it is possible to measure the height of the cloud (without reference to any external datum lines such as the artificial horizon) by using eq. (2) and measuring the distance from the cloud summit to the ground directly beneath. (The effect of refraction is to lift the ground and storm base by about 2000 ft.) Thus, knowing h, we may now obtain α from eq. (3) and so determine the position of the 0° altitude line. The distance, ξ, between this line and the visible horizon is measured, and a revised focal length F_R derived from the equation.

$$2\xi + HH = \pi F_R \qquad (4)$$

This assumes ξ is the same at both horizons. This is not necessarily so because the depression of the visible horizon below the 0° altitude level varies with the opacity of the atmosphere and may be different in different directions. It is never possible to see the land horizon, and the distance HH suggests the visible horizon is a haze top near or at the tropopause. However, the distance HH varies very little over the whole series of film, which suggests eq. (4) can be used with reasonable confidence.

In this case $F_R = 7.70 \pm 0.03$ cm., i.e., about 1 percent different from the value quoted for this model. This revised value, F_R, was used throughout the analysis.

The probable error in determination in h_c is estimated to be:

$\pm$ 1000 ft. at D = 10 n. mi.
$\pm$ 1500 ft. at D = 20 n. mi.
$\pm$ 3000 ft. at D = 50 n. mi.

Since a resolution of about 20 ft. at 10 n. mi. is obtainable from the original film, it is clear that a large loss of potential accuracy has to be accepted in this type of analysis, which has nevertheless yielded useful information.

APPENDIX II

Discussion of Cloud Formation Seen at 2225 GMT, May 24, 1962

The remarkable feature photographed during flight over giant storm cells on May 24, 1962, is reproduced in figure 7 as a mosaic of five consecutive frames taken at 32-sec. intervals.

This, of course, is not a true mosaic, and an attempt has been made by Fitzgerald and Valovcin [3] to rectify the picture by reducing all features to a common level 15,000 ft. below the aircraft. While it is obvious that there are fluctuations of a few thousand feet in the level of the visible cloud surface, this procedure is to be recommended as giving a first order idea of the features of the cloud structure in plan view. It can, however, be misleading, and particularly open to question is Fitzgerald and Valovcin's interpretation of the rippled structure above the center of the middle frame as the walls of a vortex, and we begin by looking at this interpretation.

We take as our starting point the regions of the edges of adjacent frames in the mosaic which appear to match. This is not possible on all frames because of cloud evolution in 32 sec., but where such regions can be identified, they are 3.55 n. mi. from the aircraft (distance flown in 32 sec.). Their height can be estimated, and all such regions appear to fall between 51,000 and 54,000 ft., i.e., between 15,000 and 12,000 ft. below the aircraft. Hence we have attempted an independent rectification (fig. 10) reduced to a plane at 54,000 ft.

The sun's altitude and bearing was 29° and 269° at the time of the photographs and the aircraft heading 335°; thus we can locate the antisolar point, A, on each frame.

The overall impression of figure 7 is that of a giant dome some 7 to 8 n. mi. in diameter partly obscured by cirrus. Taken by itself, frame 173 suggests a vortex formation, strengthened by shadowed region just above the center of the frams. This shadow, however, is scarcely detectable on a negative.

However, it seems to the author that the ripples could also be interpreted as a considerably foreshortened view of a sloping dome of ripples of about the same dimensions (1/4 mi. wavelength) as the broad ripples in frame 172, particularly as the latter appear to be on the same general curve. The dome interpretation is further strengthened by a distinct temperature minimum recorded by the radiometer near the time of frame 173, and to some extent by the way in which the ripples in frame 173 are illuminated.

However, if these ripples were equi-distant, the angle subtended by a ripple should increase toward the center of the photograph, whereas in fact this angle appears to remain roughly constant suggesting the ripples decrease in size toward the tower center. This, however, could be consistent with possible strong horizontal divergence in the dome surface.

Thus it is suggested the formation is probably a flat dome (forming the summit of a great quasi-steady updraught) with an initial slope at its base of 10^{o} or less, although there is not enough information to settle the issue definitely.

Finally, there is a faint rather indefinite suggestion of a spiral structure in the cloud ridges surrounding the dome which could suggest the presence of a slow rotation of the whole system.

APPENDIX III

Synoptic Notes

Figure 15 gives a summary of the main surface synoptic features in the vicinity of each storm.

All the squall lines observed in the 1962 flights lay on or near well marked dry lines, and all appeared to reach full vertical development except the storms on the squall line of May 31, 1962. The only obvious difference in the synoptic pattern was that the middle and upper troposheric winds on May 31, 1962, were backed to due S by a small cold pool[4], whereas on the other occasions, these winds were generally near WSW in direction.

In 1963, on the other hand, the dry line appeared to be farther west than usual - possibly connected with the deeper moist layer apparent on most ascents - and all storm areas investigated were about 100 (and in one case 200) n. mi. east of the dry line. On three flights the storms appeared to be of air-mass type, as no organization of their distribution was apparent, and did not realize their potential vertical extent.

There was a distinct squall line on May 31, 1963, although the organization and density of storm cells was weaker than in the 1962 flights.

---

[4] Suggesting that differential advection was greatly reduced as a result, thus reducing flux of air into storm cells.

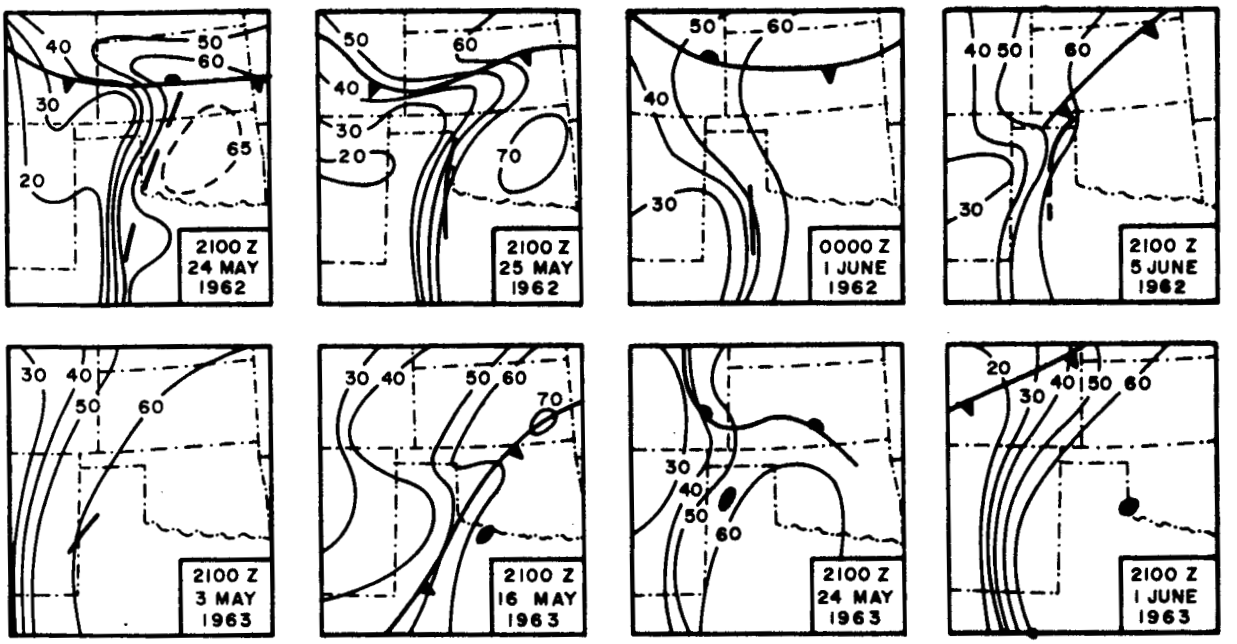

Figure 15. Summary of synoptic features associated with each flight period. ———— isopleths of dewpoint (°F); squall line; area of storms; surface front; - — - — state boundaries.

The ascents in general showed the moist layer was less moist (wet bulb potential temperature, θ_w = 20-22°C.) than in 1962 (θ_w = 22-24°C.) although deeper.

No. 27 Statistical Properties of Radar Echo Patterns and the Radar Echo Process. Larry Armijo. May 1966. The Role of the Kutto-Joukowski Force in Cloud Systems with Circulation. J. L. Goldman. May 1966.

No. 28 Movement and Predictability of Radar Echoes. James Warren Wilson. November 1966.